Inorganic Chemistry

Article

pubs.acs.org/IC

Synthesis and Characterization of Pt(II) Complexes with Pyridyl Ligands: Elongated Octahedral Ion Pairs and Other Factors Influencing ^{1}H NMR Spectra

Nerissa A. Lewis, Svetlana Pakhomova, Patricia A. Marzilli, and Luigi G. Marzilli*

Department of Chemistry, Louisiana State University, Baton Rouge, Louisiana 70803, United States

Supporting Information

ABSTRACT: Our goal is to develop convenient methods for obtaining *trans*-[Pt^{II}(4-Xpy)$_2Cl_2$] complexes applicable to 4-substituted pyridines (4-Xpy) with limited volatility and water solubility, properties typical of 4-Xpy, with X being a moiety targeting drug delivery. Treatment of *cis*-[$Pt^{II}(DMSO)_2Cl_2$] (DMSO = dimethyl sulfoxide) with 4-Xpy in acetonitrile allowed isolation of a new series of simple *trans*-[Pt^{II}(4-Xpy)$_2Cl_2$] complexes. A side product with very downfield H2/6 signals led to our synthesis of a series of new [Pt^{II}(4-Xpy)$_4$]Cl_2 salts. For both series in $CDCl_3$, the size of the H2/6 $\Delta\delta$ [coordinated minus "free" 4-Xpy H2/6 shift] decreased as 4-Xpy donor ability increased from 4-CNpy to 4-Me_2Npy. This finding can be attributed to the greater synergistic reduction in the inductive effect of the Pt(II) center with increased 4-Xpy donor ability. The high solubility of [Pt^{II}(4-Xpy)$_4$]Cl_2 salts in $CDCl_3$ (a solvent with low polarity) and the very downfield shift of the [Pt^{II}(4-Xpy)$_4$]Cl_2 H2/6 signals for the solutions provide evidence for the presence of strong {[Pt^{II}(4-Xpy)$_4$]$^{2+}$,2Cl^-} ion pairs that are stabilized by multiple CH···Cl contacts. This conclusion gains considerable support from [Pt^{II}(4-Xpy)$_4$]Cl_2 crystal structures revealing that a chloride anion occupies a pseudoaxial position with nonbonding (py)C−H···Cl contacts (2.4−3.0 Å). Evidence for (py)C−H···Y contacts was obtained in NMR studies of [Pt^{II}(4-Xpy)$_4$]Y_2 salts with Y counterions less capable of forming H-bonds than chloride ion. Our synthetic approaches and spectroscopic analysis are clearly applicable to other nonvolatile ligands.

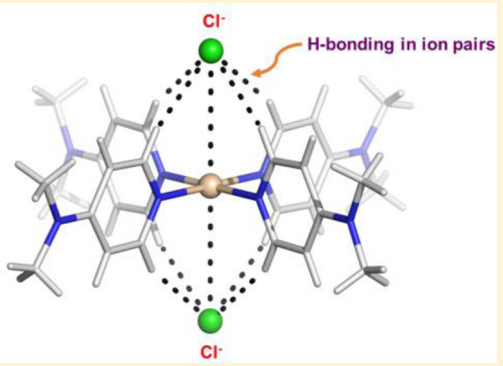

INTRODUCTION

We have been exploring the metal-binding chemistry of strongly coordinating pyridyl ligands as one means of bioconjugation of targeting biological groups to create complexes with potential therapeutic or diagnostic utility.[1] One highly useful synthon for our purposes is the C_2-symmetrical amine, 1-(4-pyridyl)piperazine (pyppzH, Figure 1). The piperazine N attached to the pyridyl ring increases the donor ability of the pyridyl ring N, whereas the remote piperazine NH group can be used for linking chemistry. In this work we pursue fundamental Pt(II) chemistry relevant to the eventual use of such bioconjugated pyridyl ligands to prepare complexes having anticancer activity.

Cisplatin, *cis*-[$Pt(NH_3)_2Cl_2$], is one of the most effective chemotherapeutic agents being used in clinical therapy.[2,3] Many closely related cis bifunctional analogues of cisplatin also show good anticancer activity.[2,4−6] In contrast, the inactivity of the *trans*-[$Pt(NH_3)_2Cl_2$] isomer has led to a presumption that trans compounds are inactive.[7−10] Historically, *trans*-[PtL_2Cl_2] complexes have been neglected. In recent years, however, several types of platinum compounds with trans geometry have shown promising in vitro activity against several cancer cell lines, including some that are resistant to cisplatin.[7−9,11−17] Among the recently studied trans platinum complexes, the iminoether complex *trans*-[Pt(*E*-HN═C(OCH_3)CH_3)$_2Cl_2$] has been studied most intensively and has demonstrated significant activity against several cisplatin-resistant tumor cell lines.[9,11,12,18] We propose that, whereas bulky ligands have been reported to decrease activity of cis bifunctional Pt(II) agents, bulky ligands are needed to allow trans bifunctional as well as monofunctional Pt(II) agents to form DNA adducts in which the DNA structure is distorted in such a way as to lead to cancer cell cytotoxicity.[19−22]

Because evidence exists that *trans*-[PtL_2Cl_2] complexes with L = 4-substituted pyridyl ligands (4-Xpy) exhibit cancer cell cytotoxicity,[16,17] we believe that 4-Xpy ligands have sufficient bulk to cause DNA distortions necessary for anticancer activity. Thus, we initiated an investigation of the preparation of *trans*-[Pt^{II}(4-Xpy)$_2Cl_2$] complexes containing strongly coordinating pyridyl ligands such as 4-piperidinopyridine (4-$(CH_2)_5$Npy, Figure 1). Syntheses reported for related complexes often yield the cis isomer, require harsh conditions (such as 100−150 °C or the use of concentrated HCl), or depend on using aqueous conditions or volatile ligands.[23−27] Such restrictions are not amenable to pyridine ligands containing sensitive linking groups, such as the sulfonamide group that we employ for bioconjugation.[28]

Received: May 19, 2017

DOI: 10.1021/acs.inorgchem.7b01294
Inorg. Chem. XXXX, XXX, XXX−XXX

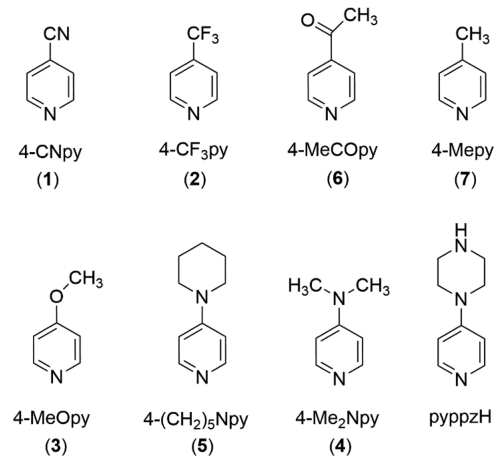

Figure 1. Pyridyl ligands (4-Xpy) used to synthesize complexes studied in the current work organized by donor ability to metals centers with the weakest donors in upper left and strongest donors in lower right. Also shown is the pyppzH synthon used in our bioconjugation approach.[1] Bold numbers below the ligands are used to designate complexes prepared with the ligand having that number. *trans*-$[Pt^{II}(4\text{-Xpy})_2Cl_2]$ complexes are designated with these bold numbers alone, and $[Pt^{II}(4\text{-Xpy})_4]Y_2$ complexes are designated with these bold numbers plus a letter that identifies the counterion Y^-, as follows: $Y^- = Cl^-$ (**a**), PF_6^- (**b**), BF_4^- (**c**), BPh_4^- (**d**), and NO_3^- (**e**). For example, $[Pt^{II}(4\text{-CNpy})_4]Cl_2$ is numbered **1a**.

In the present study, we identify versatile approaches for preparing new *trans*-$[Pt^{II}(4\text{-Xpy})_2Cl_2]$ complexes. Our syntheses do not require high temperatures or rely on using volatile or water-soluble 4-Xpy. Because the binding of purine heterocycles to Pt(II) causes ~1 ppm downfield shift changes, we expected that large downfield ^{1}H NMR shift changes of the pyridyl ^{1}H NMR signals on binding to Pt(II) would guide us in our synthetic work.[19−22,29,30] However, in our initial studies we were surprised to find only an ~0.1 ppm downfield shift change of the pyridyl H2/6 signal and even an upfield shift change of the H3/5 signal (~0.1 ppm) for ligands such as 4-$(CH_2)_5$Npy. As an aid in improving methods for the synthesis and characterization of *trans*-$[Pt^{II}(4\text{-Xpy})_2Cl_2]$ complexes, we explored fundamental features of the NMR spectra of these complexes. The relatively few known *cis/trans*-$[Pt(py)_2Y_2]$ and $[Pt(Xpy \text{ or } X_2py)_4]Y_2$ complexes (mostly with Y = halide or NCS^- and X = Me) contain ligands such as py, picolines (Mepy), and lutidines (Me_2py) of similar donor ability as estimated by the respective pK_a values of the protonated ligand, for example, $XpyH^+$, falling within a very limited pK_a range.[23,24,26,27,31−35] Also, NMR studies often were reported in different solvents.[17] Thus, the dependence of the NMR signals on the properties of the complexes, such as the pyridyl ligand donor ability, was neither well-defined nor understood. Our use of 4-Xpy ligands with substituents at ring position 4 that vary widely in donor ability (e.g., 4-CNpy and 4-Me_2Npy, Figure 1) minimizes the through-space effect of X on the H2/6 ^{1}H NMR signal. This choice allowed us to assess the through-bond inductive effect passing through the Pt(II) center on the 4-Xpy H2/6 signals for a range of *trans*-$[Pt^{II}(4\text{-Xpy})_2Cl_2]$ complexes.

During our initial investigation of *trans*-$[Pt(4\text{-Xpy})_2Cl_2]$ preparative procedures, some synthetic conditions gave side products with unprecedented, unusually downfield signals in $CDCl_3$. We identified these as H2/6 signals of $[Pt^{II}(4\text{-Xpy})_4]Cl_2$ side products. Published NMR data[23,27] for $[Pt^{II}(4\text{-Xpy})_4]Cl_2$ complexes are limited but are inconsistent with our results. To gain a comprehensive understanding of the NMR trends, we prepared a number of new $[Pt^{II}(4\text{-Xpy})_4]Y_2$ complexes with diverse 4-Xpy ligands and Y counterions. These NMR studies established that the very downfield shift position of the H2/6 pyridyl signals reflects the presence of strong $\{[Pt^{II}(4\text{-Xpy})_4]^{2+},2Cl^-\}$ ion pairs in which the H2/6 protons undoubtedly form C−H···Cl contacts. This interpretation gains support from several crystal structures of some new $[Pt^{II}(4\text{-Xpy})_4]Cl_2$ complexes. The $[Pt^{II}(4\text{-Xpy})_4]^{2+}$ cations in these crystals form part of elongated pseudo-octahedral structures with axial chloride ions that have contacts to the pyridyl ring H2/6 protons consistent with (py)C−H···Cl H-bonding interactions. The distance of the chloride counterions to the Pt(II) center is usually a few tenths of an angstrom longer than the Pt···Cl contact distance of ~3.5 Å.[36,37] Such elongated pseudo-octahedral ion pairs explain the unusual NMR features of $[Pt^{II}(4\text{-Xpy})_4]Cl_2$ complexes, and also the resulting low charge of the $\{[Pt^{II}(4\text{-Xpy})_4]^{2+},2Cl^-\}$ ion pairs is consistent with the high solubility in $CDCl_3$ of these salts containing $[Pt^{II}(4\text{-Xpy})_4]^{2+}$ cations; such salts are otherwise expected to be poorly soluble.

EXPERIMENTAL SECTION

Starting Materials. Pyridine (py), 4-cyanopyridine (4-CNpy), 4-trifluoromethylpyridine (4-CF_3py), 4-acetylpyridine (4-MeCOpy), 4-methylpyridine (4-Mepy), 4-methoxypyridine (4-MeOpy), 4-dimethylaminopyridine (4-Me_2Npy), 4-piperidinopyridine (4-$(CH_2)_5$Npy), $NaPF_6$, $[Et_4N]BF_4$, $NaBF_4$, $[Et_4N]Cl$, and $[Et_4N]NO_3$ were obtained from Sigma-Aldrich. *cis*-$[Pt^{II}(DMSO)_2Cl_2]$ was prepared by a known method.[38]

NMR Measurements. ^{1}H NMR spectra were recorded on a 400 MHz Bruker spectrometer or on an Advance-III Prodigy 500 MHz Bruker spectrometer. Peak positions are relative to 3-(trimethylsilyl)-propionic-2,2,3,3-d_4 acid in D_2O, or solvent residual peak (DMSO-d_6, CHD_2CN, or $CHCl_3$) with internal tetramethylsilane (TMS) as reference. All NMR data were processed with TopSpin and MestReNova software. For specific assignments of signals, please see Tables 1−3 and Supporting Information.

Mass Spectrometric Measurements. High-resolution mass spectra recorded on an Agilent 6210 ESI TOF LCMS mass spectrometer are reported in Supporting Information.

X-ray Data Collection and Structure Determination. Intensity data were collected at low temperature on a Bruker Kappa Apex-II

Table 1. H2/6 Chemical Shifts (ppm) and Shift Differences ($\Delta\delta$, ppm) in $CDCl_3$ at 25 °C for 4-Xpy Ligands (5 mM) Both Free and in *trans*-$[Pt(4\text{-Xpy})_2Cl_2]$ Complexes[a] (5 mM)

X	pK_a	4-Xpy	*trans*-$[Pt(4\text{-Xpy})_2Cl_2]$	H2/6 $\Delta\delta$
CN	2.10[b]	8.82	9.17	0.35
CF_3	2.46[c]	8.83	9.18	0.35
MeCO	3.51[d]	8.82	9.13	0.31
Me[e]	5.98[f]	8.47	8.71	0.24
MeO	6.47[g]	8.45	8.69	0.24
Me_2N	9.61[h]	8.22	8.35	0.13
$(CH_2)_5N$	9.60[i]	8.23	8.34	0.11

[a] *trans*-$[Pt(py)_2Cl_2]$, this study, 8.92 ppm; reported, 8.91 ppm;[23] reported for *cis*-$[Pt(py)_2Cl_2]$, 8.74 ppm.[23] [b] pK_a value from ref 52. [c] Estimated from the equation of the line: $y = -0.0884x + 9.0472$ (see Supporting Information, Figure S2). [d] pK_a value from ref 53. [e] Reported for *trans*-$[Pt(4\text{-Mepy})_2Cl_2]$, 8.69 ppm;[27] reported for *cis*-$[Pt(4\text{-Mepy})_2Cl_2]$, 8.71 ppm.[27] [f] p$K_a$ value from ref 54. [g] pK_a value from ref 55. [h] pK_a value from ref 56. [i] pK_a value from ref 1.

DOI: 10.1021/acs.inorgchem.7b01294
Inorg. Chem. XXXX, XXX, XXX−XXX

DUO CCD diffractometer fitted with an Oxford Cryostream cooler and graphite-monochromated Mo Kα (λ = 0.710 73 Å) radiation from an IμS microfocus source with multilayer optics. Data reduction included absorption corrections by the multiscan method, with SADABS.[39] All X-ray structures were determined by direct methods and difference Fourier techniques and refined by full-matrix least-squares methods by using SHELXL2014[40] with H atoms in idealized positions.

General Syntheses of *trans*-[Pt^{II}(4-Xpy)$_2$Y$_2$] and [Pt^{II}(4-Xpy)$_4$]Y$_2$ Complexes. The general synthetic method is illustrated in Scheme 1, and the numbering key for compounds in this study appears in Figure 1. Specific details on quantities used, yields, MS data, etc. can be found in Supporting Information.

Scheme 1. Synthesis of *trans*-[Pt^{II}(4-Xpy)$_2$Cl$_2$] and [Pt^{II}(4-Xpy)$_4$]Cl$_2$ Complexes,[a] Showing Numbers for Product Complexes and the Numbering System for the 4-Xpy Ligands

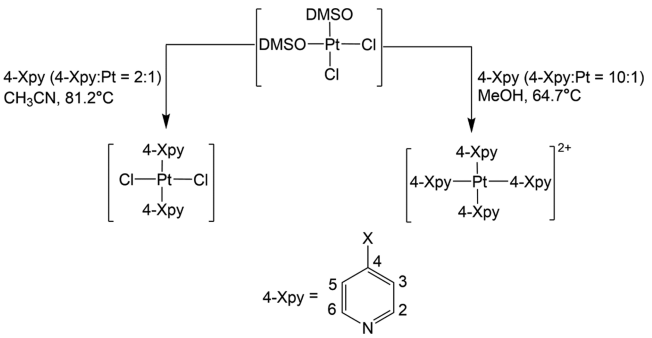

[a]Complexes that have numbers only are *trans*-[Pt(4-Xpy)$_2$Cl$_2$] complexes. Numbers correlate with ligands [X = CN (**1**); CF$_3$ (**2**); MeO (**3**); Me$_2$N (**4**); (CH$_2$)$_5$N (**5**); MeCO (**6**); and Me (**7**)].

4-Xpy was added to an acetonitrile or methanol solution of *cis*-[Pt^{II}(DMSO)$_2$Cl$_2$] (42 mg, 0.1 mmol, in 5 mL) in a 2:1 or 10:1 (4-Xpy/Pt) molar ratio, and the reaction mixture was heated at reflux for 24 h. The precipitate that formed was collected on a filter, washed with acetonitrile or methanol and diethyl ether, and dried in air. The powder collected was then dissolved in CHCl$_3$ (~1–4 mL), and diethyl ether (~10 mL) was added until cloudiness was observed. After the mixture was left undisturbed (~10–15 min at room temperature), yellow or white products were collected on a filter, washed with diethyl ether, and dried in air. Although three *trans*-[Pt^{II}(4-Xpy)$_2$Cl$_2$] complexes were previously reported [X = H,[23] MeCO,[17] and Me[24,27]], we prepared the three complexes by our synthetic method. ^{1}H NMR data at 25 °C in CDCl$_3$, CD$_3$CN, deuterated dimethyl sulfoxide (DMSO-d_6), and D$_2$O can be found in Table 1 and in the Supporting Information.

X-ray quality crystals of *trans*-[Pt^{II}(4-Xpy)$_2$Cl$_2$] (X = CF$_3$ (**2**), MeO (**3**), and (CH$_2$)$_5$N (**5**)) and [Pt^{II}(4-Xpy)$_4$]Cl$_2$ (X = MeO (**3a**), Me$_2$N (**4a**), (CH$_2$)$_5$N (**5a**), and Me (**7a**)) were obtained by mixing equal volumes (1 mL) of 4-Xpy and *cis*-[Pt^{II}(DMSO)$_2$Cl$_2$] (5.3 mg, 12.5 mM) in 2:1 or 10:1 (4-Xpy/Pt) molar ratios in acetonitrile and allowing the mixture to stand at room temperature for 4–24 d. When this room-temperature procedure was followed with 4-Me$_2$Npy (3.1 mg, 25 mM), the X-ray quality crystals collected after 8 d were the *cis*-[Pt^{II}(4-Me$_2$Npy)$_2$Cl$_2$] isomer (**4′**).

The treatment of an aqueous solution (3–5 mL) of [Pt^{II}(4-Xpy)$_4$]Cl$_2$ (X = MeO (**3a**), Me$_2$N (**4a**), (CH$_2$)$_5$N (**5a**), and Me (**7a**)) (0.1 mmol) with solid NaPF$_6$ (170 mg, 1.0 mmol), [NEt$_4$]BF$_4$ (220 mg, 1.0 mmol), or NaBPh$_4$ (0.342 g, 1.0 mmol) produced the respective [Pt^{II}(4-Xpy)$_4$](PF$_6$)$_2$ (**3b–5b** and **7b**), [Pt^{II}(4-Xpy)$_4$](BF$_4$)$_2$ (**3c–5c** and **7c**), or [Pt^{II}(4-Xpy)$_4$](BPh$_4$)$_2$ (**2d** and **4d**) complexes as white solids, which were collected on a filter, washed with diethyl ether, and dried in air.

Alternate Synthesis of [Pt^{II}(4-Xpy)$_4$]Y$_2$ Complexes (X = CN, CF$_3$, MeCO, MeOpy, or Me$_2$N; Y = NO$_3^-$, PF$_6^-$, or BF$_4^-$). The general synthetic method for [Pt^{II}(4-Xpy)$_4$]Y$_2$ complexes was not successful with weak donor ligands (4-CNpy, 4-CF$_3$py, and 4-MeCOpy). The desired [Pt^{II}(4-Xpy)$_4$]Y$_2$ complexes were prepared by an alternate method. Specific details on quantities used, yields, MS data, etc. can be found in Supporting Information. In this alternate method, a methanol solution (5 mL) of *cis*-[Pt^{II}(DMSO)$_2$Cl$_2$] (42 mg, 0.1 mmol) was first treated with AgNO$_3$ (29 mg, 0.17 mmol) and then with 4-CNpy, 4-CF$_3$py, and 4-MeCOpy in a 40:1 (4-Xpy/Pt) molar ratio. The moderate and strong donor ligands, 4-Mepy, 4-MeOpy, and 4-Me$_2$Npy, were used to prepare [Pt^{II}(4-Xpy)$_4$](NO$_3$)$_2$ complexes (**7e**, **3e**, and **4e**) for comparison to the analogues having weak 4-Xpy donors. The reaction mixture was heated at reflux for 24 h; after ~10 min a white precipitate (presumed to be AgCl) formed, and the gray precipitate produced was collected on a filter and then suspended in acetonitrile (2–4 mL) to dissolve the desired [Pt^{II}(4-Xpy)$_4$](NO$_3$)$_2$ salt. The mixture was filtered (to remove AgCl), and ether was added to the filtrate to the point of cloudiness (~10–15 mL). The white precipitate formed {[Pt^{II}(4-CNpy)$_4$](NO$_3$)$_2$ (**1e**), [Pt^{II}(4-CF$_3$py)$_4$](NO$_3$)$_2$ (**2e**), [Pt^{II}(4-MeCOpy)$_4$](NO$_3$)$_2$ (**6e**)} was collected on a filter, washed with methanol and diethyl ether, and dried in air. For all of these products, ^{1}H NMR spectra (in CD$_3$CN at 25 °C) recorded both upon dissolution and subsequently contained only one set of signals.

The treatment of an aqueous solution (3–5 mL) of [Pt^{II}(4-Xpy)$_4$](NO$_3$)$_2$ (X = CN (**1e**), CF$_3$ (**2e**), or MeCO (**6e**)) (0.1 mmol) with solid NaPF$_6$ (170 mg, 1.0 mmol) or NaBF$_4$ (110 mg, 1.0 mmol) produced the respective [Pt^{II}(4-Xpy)$_4$](PF$_6$)$_2$ (**1b**, **2b**, and **6b**) or [Pt^{II}(4-Xpy)$_4$](BF$_4$)$_2$ (**1c**, **2c**, and **6c**) as white solids, which were collected on a filter, washed with water and diethyl ether, and dried in air. [Pt^{II}(4-Xpy)$_4$](PF$_6$)$_2$ and [Pt^{II}(4-Xpy)$_4$](BF$_4$)$_2$ [X = MeO (**3b** and **3c**), Me$_2$N (**4b** and **4c**), or Me (**7b** and **7c**)] were prepared as described above by using solid [NEt$_4$]BF$_4$. ^{1}H NMR data in CDCl$_3$,

Table 2. H2/6 Chemical Shifts (ppm) and Shift Differences ($\Delta\delta$, ppm) in CDCl$_3$ at 25 °C for 4-Xpy Ligands (5 mM) Both Free and in [Pt(4-Xpy)$_4$]Y$_2$ Complexes (5 mM)

		H2/6					H2/6 $\Delta\delta$			
X/Y	pK_a	free	Cl$^-$	NO$_3^-$	BF$_4^-$	PF$_6^-$	Cl$^-$	NO$_3^-$	BF$_4^-$	PF$_6^-$
CN	2.10[a]	8.82	10.66[b]	ins	ins	ins	1.84[b]	ins	ins	ins
CF$_3$[c]	2.46[d]	8.83	10.74[b]	9.97	9.76	ins	1.91[b]	1.14	0.93	ins
MeCO	3.51[e]	8.82	10.60[b]	ins	9.62	ins	1.78[b]	ins	0.80	ins
Me	5.98[f]	8.47	10.02[g]	9.36	9.11	8.86	1.55[g]	0.89	0.64	0.39
MeO	6.47[h]	8.45	9.93[g]	9.24	9.04	8.79	1.48[g]	0.79	0.59	0.34
Me$_2$N[i]	9.61[j]	8.22	9.07[g]	8.66	8.49	8.24	0.85[g]	0.44	0.27	0.02
(CH$_2$)$_5$N	9.60[1k]	8.23	9.00[g]		8.44	8.22	0.77[g]		0.21	−0.01

[a]pK_a value from ref 52. [b]Contains 50 mM [Et$_4$N]Cl. [c][Pt(4-CF$_3$py)$_4$](BPh$_4$)$_2$ is insoluble in CDCl$_3$ at 25 °C. [d]Estimated from the equation of the line: $y = -0.0884x + 9.0472$ (see Supporting Information, Figure S2). [e]pK_a value from ref 53. [f]pK_a value from ref 54. [g]Contains 40 mM [Et$_4$N]Cl. [h]pK_a value from ref 55. [i][Pt(4-Me$_2$Npy)$_4$](BPh$_4$)$_2$, 7.28 ppm. [j]pK_a value from ref 56. [k]pK_a value from ref 1.

DOI: 10.1021/acs.inorgchem.7b01294
Inorg. Chem. XXXX, XXX, XXX–XXX

Table 3. H2/6 Chemical Shifts (ppm) and Shift Differences ($\Delta\delta$, ppm) in CD_3CN at 25 °C for 4-Xpy Ligands (5 mM) Both Free and in $[Pt(4\text{-Xpy})_4]Y_2$ Complexes (5 mM)

		H2/6					H2/6 $\Delta\delta$			
X/Y	pK_a	free	Cl^-	NO_3^-	BF_4^-	PF_6^-	Cl^-	NO_3^-	BF_4^-	PF_6^-
CN	2.10[a]	8.78	10.50[b]	9.31	9.01	8.93	1.72[b]	0.53	0.23	0.15
CF_3[c]	2.46[d]	8.82	10.59[b]	9.45	9.07	9.02	1.77[b]	0.63	0.25	0.20
MeCO	3.51[e]	8.77	10.51[b]	9.28	8.97	8.95	1.74[b]	0.51	0.20	0.18
Me	5.98[f]	8.41	9.84[g]	8.63	8.50	8.48	1.43[g]	0.22	0.09	0.07
MeO	6.47[h]	8.38	9.83[g]	8.59	8.40	8.37	1.45[g]	0.21	0.02	−0.01
Me_2N[i,j]	9.61[k]	8.13	8.75[g]	8.00	7.91	7.90	0.62[g]	−0.13	−0.22	−0.23
$(CH_2)_5N$	9.60[l]	8.13	8.74[g]		7.88	7.85	0.61[g]		−0.25	−0.28

[a] pK_a value from ref 52. [b] Contains 50 mM $[Et_4N]Cl$. [c] $[Pt(4\text{-}CF_3py)_4](BPh_4)_2$, 9.01 ppm. [d] Estimated from the equation of the line: $y = -0.0884x + 9.0472$ (see Supporting Information, Figure S2). [e] pK_a value from ref 53. [f] pK_a value from ref 54. [g] Contains 40 mM $[Et_4N]Cl$. [h] pK_a value from ref 55. [i] Data collected for $[Pt(4\text{-}Me_2Npy)_4]Cl_2$ (without $[Et_4N]Cl$), 8.42 ppm. [j] $[Pt(4\text{-}Me_2Npy)_4](BPh_4)_2$, 7.88 ppm. [k] pK_a value from ref 56. [l] pK_a value from ref 1.

DMSO-d_6, D_2O, and CD_3CN at 25 °C appear in Tables 2 and 3 and in Supporting Information.

$[Et_4N]Cl$ Addition to $[Pt^{II}(4\text{-Mepy})_4](NO_3)_2$, $[Pt^{II}(4\text{-Mepy})_4](BF_4)_2$, and $[Pt^{II}(4\text{-Xpy})_4](PF_6)_2$ Complexes (X = Me, MeO, Me_2N, and $(CH_2)_5N$) in $CDCl_3$ or DMSO-d_6. The effect of $[Et_4N]Cl$ on a 5 mM solution of the desired $[Pt^{II}(4\text{-Xpy})_4]Y_2$ complex in $CDCl_3$ (except for $[Pt^{II}(4\text{-}Me_2Npy)_4](PF_6)_2$, which was poorly soluble) or DMSO-d_6 was studied with a 600 mM stock solution of $[Et_4N]Cl$ prepared from a 5 mM solution of the complex to keep the complex concentration constant throughout the experiment. ^1H NMR spectra were recorded for each solution (1−125 mM in $[Et_4N]Cl$) after the addition of each $[Et_4N]Cl$ aliquot. As the Cl^- concentration was increased from 0−125 mM, a downfield shift (0.05 ppm) was observed for the residual $CHCl_3$ signal (from 7.2629 to 7.3080 ppm) relative to TMS as reference. To account for this shift change, shifts of all peaks were adjusted accordingly.

$[Et_4N]Cl$ Addition to $[Pt^{II}(4\text{-Xpy})_4](NO_3)_2$ in $CDCl_3$ or CD_3CN. NMR tubes containing enough solid $[Pt^{II}(4\text{-Xpy})_4](NO_3)_2$ (X = CN or CF_3) and $CDCl_3$ (600 μL) to make 5 mM solutions in $CDCl_3$ at 25 °C were treated with enough $[Et_4N]Cl$ (12.4 mg) to make a 125 mM solution. The two salts dissolved rapidly, and ^1H NMR spectra were recorded for each solution within a few minutes and over a period of 9 d. Because of the low solubility of these $[Pt^{II}(4\text{-Xpy})_4](NO_3)_2$ (X = CN or CF_3) salts in $CDCl_3$, we studied them (as well as nitrate salts having moderate and good donor 4-Xpy ligands) in CD_3CN, by recording ^1H NMR spectra soon after and 24 h after addition of 10 molar equiv of $[Et_4N]Cl$ (5 mg).

$[Et_4N]Cl$ Addition to $[Pt^{II}(4\text{-Xpy})_4]Y_2$ Complexes in D_2O or DMSO-d_6. Solutions (5 mM) of selected $[Pt^{II}(4\text{-Xpy})_4]Y_2$ complexes in D_2O or DMSO-d_6 (600 μL) at 25 °C were treated with 10 molar equiv of $[Et_4N]Cl$ (5 mg) for $[Pt^{II}(4\text{-Xpy})_4](NO_3)_2$ salts or with 8 molar equiv of $[Et_4N]Cl$ (4 mg) for $[Pt^{II}(4\text{-Xpy})_4]Cl_2$ salts; each solution was examined by ^1H NMR spectroscopy.

RESULTS AND DISCUSSION

Synthesis. As illustrated in Scheme 1, the treatment of *cis*-$[Pt^{II}(DMSO)_2Cl_2]$ in acetonitrile with 2 equiv of 4-Xpy afforded 26−51% yields of solids containing pure *trans*-$[Pt^{II}(4\text{-Xpy})_2Cl_2]$ complexes (X = CN, CF_3, MeCO, Me, MeO, and $(CH_2)_5N$). However, when methanol was used as the solvent, mixtures of cis and trans isomers of $[Pt^{II}(4\text{-Xpy})_2Cl_2]$ were obtained, as could be deduced from reported NMR data[23,24,27] on a few $[Pt^{II}(4\text{-Xpy})_2Cl_2]$ complexes; in addition, spectra showed small signals with very downfield shifts that did not correspond to those in any literature reports.

When a methanol solution of *cis*-$[Pt^{II}(DMSO)_2Cl_2]$ was treated instead with 10 equiv of relatively good 4-Xpy donor ligands (X = Me, MeO, Me_2N, and $(CH_2)_5N$), $[Pt^{II}(4\text{-Xpy})_4]Cl_2$ complexes were formed in 49−84% yields. These dicationic complexes were very soluble in $CDCl_3$ and exhibited the unusual, very downfield minor H2/6 NMR signals observed in reactions with only 2 equiv of 4-Xpy. Factors leading to the high solubility and very downfield shifts are discussed below.

To expand the range of 4-Xpy basicity and donor ability in the $[Pt^{II}(4\text{-Xpy})_4]Y_2$ series, a modified synthetic approach was employed. When 4-CNpy, 4-CF_3py, or MeCO was added to a methanol solution of *cis*-$[Pt^{II}(DMSO)_2Cl_2]$ in a 40:1 (4-Xpy/Pt) molar ratio and the solution heated to reflux in the presence of $AgNO_3$, the respective $[Pt^{II}(4\text{-Xpy})_4](NO_3)_2$ complexes were obtained in 68%, 87%, or 76% yields. Aqueous solutions of $[Pt^{II}(4\text{-Xpy})_4](NO_3)_2$ (X = CN (**1e**), CF_3 (**2e**), and MeCO (**6e**) and $[Pt^{II}(4\text{-Xpy})_4]Cl_2$ (X = MeO (**3a**), Me_2N (**4a**), $(CH_2)_5N$ (**5a**), and Me (**7a**)) (0.1 mmol) were then treated with solid $NaPF_6$, $NaBF_4$, or $[Et_4N]BF_4$ to produce the respective $[Pt^{II}(4\text{-Xpy})_4](PF_6)_2$ (**1b**−**7b**) or $[Pt^{II}(4\text{-Xpy})_4](BF_4)_2$ (**1c**−**7c**) complexes.

Structural Results. Overall Aspects. Crystal data and details of the structural refinement for complexes **2**, **3**, **4′**, **5**, **3a**−**5a**, and **7a** are summarized in Supporting Information; ORTEP plots for these compounds are shown in Figures 2−4, along with the atom-numbering schemes used to describe the solid-state data. Selected bond lengths and bond angles are presented in Tables 4−6. In the *trans*-$[Pt^{II}(4\text{-Xpy})_2Cl_2]$ complexes (**2**, **3**, and **5**), the Pt^{II} metal center has two trans chloro ligands and two N-bonded pyridyl ligands (Figure 2).

$[Pt^{II}(4\text{-Xpy})_2Cl_2]$ Structures. Even though the 4-Xpy ligands differ considerably in donor potential, the values of the Pt−N, Pt−Cl, C1−N1, and C5−N1 bond distances and the Pt−N−C and C−N−C bond angles for *trans*-$[Pt^{II}(4\text{-Xpy})_2Cl_2]$, X = CF_3 (**2**), MeO (**3**), and $(CH_2)_5N$ (**5**) (Table 4) and for *cis*-$[Pt^{II}(4\text{-}Me_2Npy)_2Cl_2]$ (**4′**) (Table 5) are not significantly different. In addition, no significant differences were observed in the metrics of the molecular structure of these new structures with those reported for *trans*-$[Pt^{II}(py)_2Cl_2]$[41] and *cis*-$[Pt^{II}(py)_2Cl_2]$[41] or for *trans*-$[Pt^{II}(4\text{-Mepy})_2Cl_2]$[24] and *cis*-$[Pt^{II}(4\text{-Mepy})_2Cl]$.[24] Thus, these structural parameters are not significantly influenced by either the basicity of 4-Xpy or the cis or trans geometry of the complex. In the $[Pt^{II}(4\text{-Xpy})_2Cl_2]$ complexes studied here, the dihedral angle between the plane of the 4-substituted pyridine ligands and the coordination plane (a feature we call canting) is ∼50° (see Supporting Information).

$[Pt^{II}(4\text{-Xpy})_4]Cl_2$ Structures. ORTEP plots for the cations of $[Pt^{II}(4\text{-MeOpy})_4]Cl_2$ (**3a**), $[Pt^{II}(4\text{-}Me_2Npy)_4]Cl_2$ (**4a**), $[Pt^{II}(4\text{-}(CH_2)_5Npy)_4]Cl_2$ (**5a**), and $[Pt^{II}(4\text{-Mepy})_4]Cl_2$ (**7a**)

DOI: 10.1021/acs.inorgchem.7b01294
Inorg. Chem. XXXX, XXX, XXX−XXX

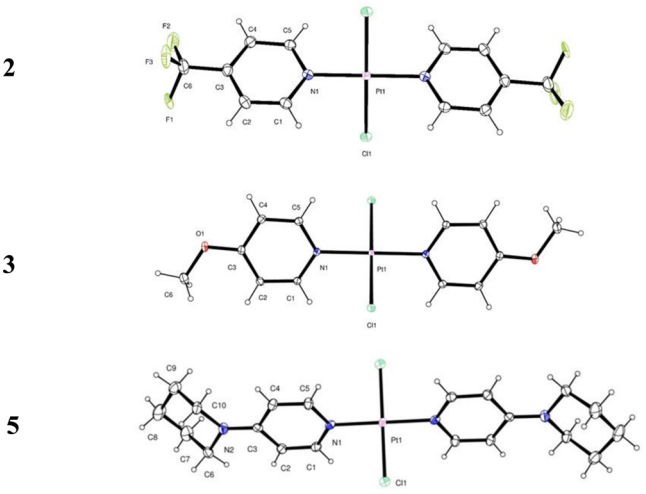

Figure 2. ORTEP plots of *trans*-[Pt(4-CF_3py)$_2$$Cl_2$] (**2**), *trans*-[Pt(4-MeOpy)$_2$$Cl_2$] (**3**), and *trans*-[Pt(4-$(CH_2)_5$Npy)$_2$$Cl_2$] (**5**). Thermal ellipsoids are drawn with 50% probability. The asymmetric unit has only half of each molecule. For the figure, the other half of each structure was generated by using the inversion center. The trifluoromethyl group in **2** is disordered over three positions; only one position is shown for clarity.

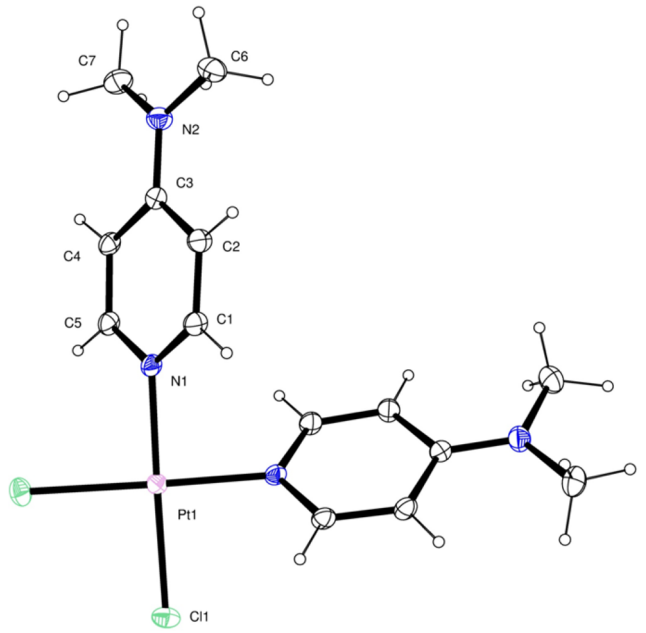

Figure 3. ORTEP plot of *cis*-[Pt(4-Me_2Npy)$_2$$Cl_2$] (**4′**). Thermal ellipsoids are drawn with 50% probability. The asymmetric unit has only half of a molecule. For the figure, the other half of the structure was generated by a twofold rotational axis.

are shown in Figure 4. The asymmetric unit of **4a** has two independent molecules (A and B), one of which lies on an inversion center. Two independent molecules are also found in the asymmetric unit of **5a**, both of them lying on an inversion center. The molecular structure of **7a** has a twofold axis through the central Pt atom.

The Pt−N and C−N bond distances and the C−N−C, C−N−Pt, and N−Pt−N bond angles (Table 6) all suggest very similar binding of the 4-Xpy ligands in the $[Pt^{II}(4\text{-Xpy})_4]^{2+}$ cation of **3a**, **4a**, **5a**, and **7a**, with N−Pt−N bond angles close to 180°. In general, the Pt−N bond distances for $[Pt^{II}(4\text{-Xpy})_4]^{2+}$ (X = MeO (**3a**), Me_2N (**4a**), $(CH_2)_5N$ (**5a**), and Me (**7a**)) (Table 6) compare well with other Pt−N(sp^2) bond distances ranging from 1.99 to 2.08 Å.[22,42,43] The canting angle for $[Pt^{II}(4\text{-Xpy})_4]^{2+}$ cations varies from ∼89.2° in **4a** to ∼76.4° in **5a**, indicating less canting than in *trans*-$[Pt^{II}(4\text{-Xpy})_2Cl_2]$ compounds. The large differences in the canting angles indicate that there is a very low barrier preventing changes in the dihedral angle.

Pt···Cl and CH···Cl Nonbonded Distances in $[Pt^{II}(4\text{-Xpy})_4]Cl_2$ (X = MeO (3a), Me_2N (4a), $(CH_2)_5N$ (5a), or Me (7a)) Crystals. In almost all cases, the chloride counterions of the new crystals lie along pseudoaxial sites of the Pt(II) center but usually at distances that are a few tenths of an angstrom longer than the Pt···Cl contact distance of ∼3.5 Å.[36,37] Including the two counterions and the cation, we can describe the configuration as resembling an axially elongated octahedron for both independent molecules in $[Pt^{II}(4\text{-}(CH_2)_5Npy)_4]Cl_2\cdot 4H_2O$ (**5a**) (in which Pt atoms occupy inversion centers with Pt···Cl distances of 3.885 and 3.912 Å for the A and B molecules, respectively; see Supporting Information, Table S3) and Molecule B of $[Pt^{II}(4\text{-}Me_2Npy)_4]Cl_2$ (**4a**) (with the Pt atom at an inversion center and the Pt···Cl distance = 3.793 Å). Molecule A of **4a**, the Pt atom has an elongated pseudo square pyramidal arrangement (Pt···Cl distance is 3.675 Å), a structure serving as a model for $\{[Pt^{II}(4\text{-Xpy})_4]^{2+},Cl^-\}^+$ ion pairs with only one chloride present in solutions made with moderately polar solvents such as CD_3CN (see below). The axially elongated octahedral arrangement in $[Pt^{II}(4\text{-Mepy})_4]Cl_2\cdot H_2O$ (**7a**) is less regular and lacks an inversion center; the two Cl^- anions nearest to Pt lie along the twofold rotational axis perpendicular to the Pt coordination plane, forming a pseudo-octahedral arrangement with slightly differing Pt···Cl nonbonded distances of 3.470 Å (Cl1) and 3.690 Å (Cl2) (see Supporting Information, Table S3). In $[Pt^{II}(4\text{-MeOpy})_4]Cl_2$ (**3a**), there are disordered Cl^- anions, precluding detailed geometric comparison of the arrangement of the Cl^- anions relative to the cation; however, the elongated pseudo-octahedral arrangement appears to be present in this case also. Finally, although this topic was neither noted nor discussed in the report of the structure of $[Pt^{II}(py)_4]Cl_2$ (**8a**), the structure does have axially located chlorides (Pt···Cl distance 3.631 Å).[44]

In the structures of **4a**, **5a**·$4H_2O$, and **7a**·H_2O, the distance between many of the pyridyl H2/6 protons and the Cl^- counteranions are short enough to be considered as a CH···Cl intermolecular contact.[45] The contacts for **4a** are shown in Figure 5. Although invariably weak, such contacts are known to exhibit the characteristics of conventional hydrogen bonds,[45−47] to occur widely in crystals,[46,48] and possibly to extend beyond the 3.0 Å van der Waals separation.[48] The CH···Cl intermolecular contacts can be described as short (<2.6 Å, ($d \ll \sum_{vdW}$), medium (2.6−3.0 Å, ($d \leq \sum_{vdW}$), or long (>3.0 Å, ($d > \sum_{vdW}$).[46]

The four nonbonding (py)C−H···Cl distances found in each structure range from 2.711 to 2.884 Å and from 2.802 to 2.980 Å for molecules A and B, respectively, of **4a**, from 2.718 to 3.171 Å and from 2.807 to 3.111 Å for molecules A and B, respectively, of **5a**·$4H_2O$, and from 2.702 to 2.814 Å for **7a**·H_2O (see Supporting Information, Table S3). Most of these contacts are in the medium range. The nonbonding (py)C−H···Cl distances observed for **7a**·H_2O (bearing the least basic 4-Mepy ligand in the structures obtained here) have an average = 2.761 Å, a value which is slightly shorter than the averages for

DOI: 10.1021/acs.inorgchem.7b01294
Inorg. Chem. XXXX, XXX, XXX−XXX

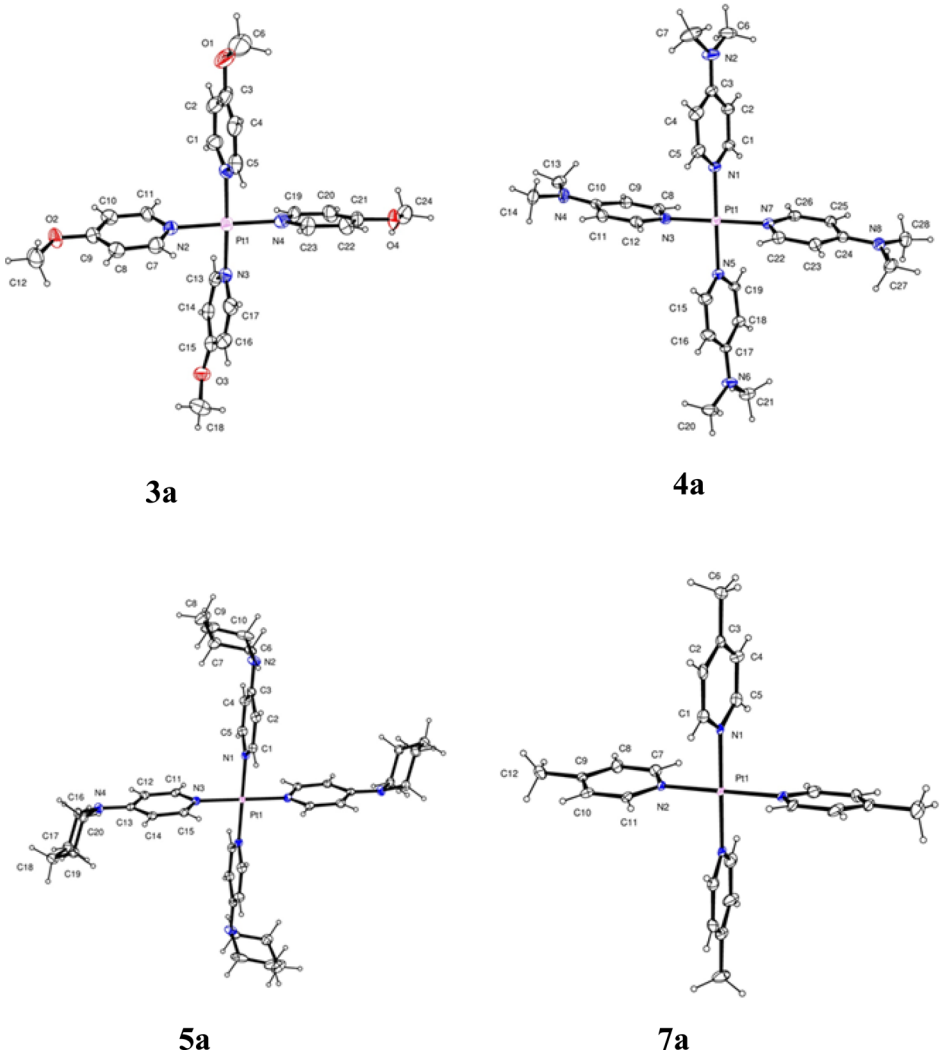

Figure 4. ORTEP plots of the cations of $[Pt(4\text{-}MeOpy)_4]Cl_2$ (**3a**), $[Pt(4\text{-}Me_2Npy)_4]Cl_2$ (**4a**), $[Pt(4\text{-}(CH_2)_5Npy)_4]Cl_2$ (**5a**), and $[Pt(4\text{-}Mepy)_4]Cl_2$ (**7a**). Thermal ellipsoids are drawn with 50% probability.

Table 4. Selected Bond Distances (Å) and Angles (deg) for *trans*-$[Pt(4\text{-}Xpy)_2Cl_2]$ [X = CF_3 (2), MeO (3), $(CH_2)_5N$ (5), H, and Me] Complexes

	CF_3[a]	MeO[a]	$(CH_2)_5N$[a]	H[b]	Me[b]
		bond distances			
Pt1−N1	2.0094(19)	2.0283(13)	2.026(2)	1.977	2.024
Pt1−Cl1	2.3005(5)	2.3000(4)	2.2998(7)	2.308	2.305
C1−N1	1.350(3)	1.3473(19)	1.335(3)	1.370	1.333
C5−N1	1.350(3)	1.351(2)	1.350(3)	1.408	1.348
		bond angles			
N1−Pt1−Cl1	90.24(5)	90.34(4)	90.52(7)	91.99	89.80
N1−Pt1−Cl1	89.76(5)	89.66(4)	89.48(7)	91.99	89.80
N1−Pt1−N1	180.0	180.0	180.0	180.00	180.00
Cl1−Pt1−Cl1	180.0	180.0	180.0	180.00	180.00
Pt1−N1−C1	121.12(16)	121.71(10)	121.03(17)	123.89	120.00
Pt1−N1−C5	119.82(16)	120.65(10)	121.38(18)	120.36	121.00
C1−N1−C5	119.0(2)	117.63(13)	117.6(2)	115.50	118.3(5)

[a]Pt atom occupies an inversion center (half of the molecule is generated by an inversion center). [b]Data for X = H (refs 24 and 41) and Me (ref 24) are obtained from the literature, and no standard deviation was obtained from the database.

4a (2.851 Å) and for **5a**·$4H_2O$ (2.954 Å), the complexes with the highly basic 4-Me_2Npy and 4-$(CH_2)_5$Npy ligands, respectively. This trend is expected and can be attributed to the higher $\delta+$ charge on the (py)C−H protons of 4-Mepy (**7a**·H_2O), which leads to stronger CH···Cl intermolecular interactions and thus shorter (py)C−H···Cl contacts. All of the $[Pt^{II}(4\text{-}Xpy)_4]Cl_2$ crystals obtained in this study have relatively good 4-Xpy donors. For the analogues with weaker

DOI: 10.1021/acs.inorgchem.7b01294
Inorg. Chem. XXXX, XXX, XXX−XXX

Table 5. Selected Bond Distances (Å) and Angles (deg) for *cis*-$[Pt(4\text{-}Me_2Npy)_2Cl_2]$[a] (4′)

	bond distances
Pt1−N1	2.0217(10)
Pt1−Cl1	2.3028(3)
C1−N1	1.3500(15)
C5−N1	1.3569(14)
	bond angles
$N1^i$−Pt1−N1	88.47(6)
$N1^i$−Pt1−$Cl1^i$	178.40(3)
$N1^i$−Pt1−Cl1	90.26(3)
$Cl1^i$−Pt1−Cl1	91.020(17)
Pt1−N1−C1	122.57(7)
Pt1−N1−C5	120.41(8)
C1−N1−C5	116.81(10)

[a]Symmetry operator (i) = $-x + 1, y, -z + 3/2$.

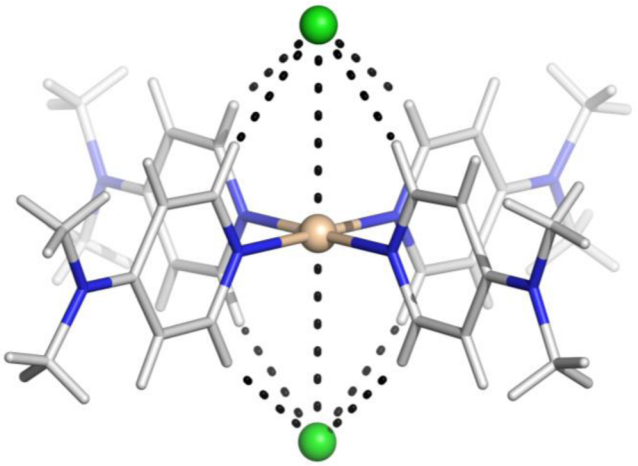

Figure 5. Pseudo-elongated octahedral geometry in $[Pt(4\text{-}Me_2Npy)_4]Cl_2$ (**4a**) formed by nonbonding (py)C−H···Cl interactions between the aromatic protons closest to the platinum atom and the two nearest Cl^- anions.

donor 4-Xpy ligands (X = CN, CF_3, and MeCO), the chloride displaces the 4-Xpy ligand, as discussed below, precluding the isolation of crystals. However, we expect that the (py)C−H···Cl contacts for complexes possessing less basic 4-Xpy donors would be shorter than those observed here for **4a**, **5a**·$4H_2O$, and **7a**·H_2O.

NMR Spectroscopy. Selected ^1H NMR spectroscopic data for 4-Xpy ligands and complexes, including the H2/6 (more downfield) and H3/5 aromatic ^1H NMR signals assigned in accordance with the widely observed pattern,[1,49] are collected in Tables 1−3 and in the Supporting Information. The atom-

Table 6. Selected Bond Distances (Å) and Angles (deg) for $[Pt(4\text{-}Xpy)_4]Cl_2$ [X = MeO (3a), Me_2N (4a), $(CH_2)_5N$ (5a), and Me (7a)] Complexes[a]

	3a	4a (A)	4a (B)	5a (A)	5a (B)	7a
			bond distances			
Pt1−N1	2.014(8)	2.020(4)	2.008(5)	2.014(2)	2.010(2)	2.016(5)
Pt1−N2	2.027(9)	2.011(5)				2.033(6)
Pt1−N(m)[a]	2.026(9)[b]	2.016(4)[b]	2.026(4)[b]	2.021(2)[b]	2.005(2)[b]	
Pt1−N(n)[a]	2.008(9)[c]	2.013(5)[c]				
			bond angles			
N1−Pt1−N(m)	177.9(3)[b]	179.32(17)[b]	180.0(0)[d]	180.0(0)[d]	180.0(0)[d]	179.6(3)[d]
N2−Pt1−N(n)	179.0(4)[c]	178.95(18)[c]				179.3(3)[e]
N1−Pt1−N2	89.8(3)	88.12(18)				90.3(2)
N1−Pt1−N(m)			92.11(19)[b], 87.89(19)[b]	92.51(9)[b], 87.49(9)[b]	91.56(9)[b], 88.44(9)[b]	
N1−Pt1−N(n)	91.1(4)[c]	92.23(18)[e]				89.7(2)[e]
N2−Pt1−N(m)	88.3(3)[b]	92.42(18)[b]				
N(m)−Pt1−N(m)			180.0(0)[b]	180.0(0)[b]		
N1−Pt1−N(m)					180.0(0)[b]	
N(m)−Pt1−N(n)	90.8(4)[b,c]	87.22(18)[b,c]				
C1−N1−C5	118.7(10)	117.3(5)	117.5(5)	117.3(3)	117.4(2)	118.6(6)
C1−N1−Pt1	120.4(7)	122.0(4)	122.2(4)	120.33(19)	121.17(19)	120.7(5)
C5−N1−Pt1	120.8(8)	120.7(4)	120.2(4)	122.3(2)	121.5(2)	120.8(5)
C7−N2−C11	118.5(10)					119.1(6)
C11−N2−C15						
C11−N(m)−C15				117.4(2)[b]	116.9(2)[b]	
C7−N2−Pt1	120.6(7)					120.1(5)
C8−N2−C12		116.7(5)				
C8−N2−Pt1		120.0(4)				
C8−N(m)−Pt1			121.5(4)[b]			
C11−N2−Pt1	120.9(7)					120.8(5)
C11−N(m)−Pt1				121.66(19)[b]	121.0(2)[b]	
C12−N2−Pt1		122.8(4)				
C12−N(m)−Pt1			120.6(4)			
C15−N2−Pt1						
C15−N(m)−Pt1				120.78(19)	122.05(19)[b]	

[a]m and n vary according to the R group. [b]m = 3. [c]n = 4. [d]m = 1. [e]n = 2.

DOI: 10.1021/acs.inorgchem.7b01294
Inorg. Chem. XXXX, XXX, XXX−XXX

numbering system used in this NMR discussion is shown in Scheme 1.

Previous limited NMR studies on *cis*/*trans*-$[Pt^{II}(py)_2Cl_2]$ and *cis*/*trans*-$[Pt^{II}(4\text{-Xpy})_2Cl_2]$ complexes employed pyridine-type ligands having properties in a narrow range.[23−25,27,33] In $CDCl_3$, the H2/6 signal of py in *trans*-$[Pt^{II}(py)_2Cl_2]$ was shifted downfield by ∼0.3 ppm as compared to free ligand[24] (see footnotes in Table 1 and Supporting Information, Table S5); this characteristic downfield chemical shift change giving a positive value for the parameter $\Delta\delta$ ($\Delta\delta = \delta_{complex} - \delta_{ligand}$) is approximately the expected value[24] and is usually interpreted as resulting from the decrease in the electron density of the ligand upon coordination.[17,24,27]

In the present study, we first examined relatively basic ligands that can be used in our bioconjugation approach and found that the *trans*-$[Pt^{II}(4\text{-Xpy})_2Cl_2]$ products had rather small H2/6 $\Delta\delta$ values in $CDCl_3$ (∼0.1 ppm). This H2/6 $\Delta\delta$ value is comparable to that reported for the $[Pt^{II}(py)_2Cl_2]$ cis isomer (∼0.1 ppm) as compared to the trans isomer (∼0.3 ppm).[23,24] The smaller H2/6 $\Delta\delta$ value for *cis*-$[Pt^{II}(py)_2Cl_2]$ versus *trans*-$[Pt^{II}(py)_2Cl_2]$ was attributed to the mutual anisotropic shielding effect exerted by adjacent cis anisotropic py ligands.[23,27] Thus, the NMR data do not provide a very useful guide in synthetic studies of *trans*-$[Pt^{II}(4\text{-Xpy})_2Cl_2]$ complexes. In addition, we also observed side products having very downfield H2/6 signals. Thus, to understand the factors that influence H2/6 $\Delta\delta$ values, we prepared and examined complexes of 4-Xpy ligands having a wide range of donor ability.

***trans*-$[Pt^{II}(4\text{-Xpy})_2Cl_2]$ Complexes.** As expected, coordination of 4-Xpy to form *trans*-$[Pt^{II}(4\text{-Xpy})_2Cl_2]$ complexes led to positive $\Delta\delta$ values for the H2/6 signal (Table 1). For both the free 4-Xpy ligands and the *trans*-$[Pt^{II}(4\text{-Xpy})_2Cl_2]$ complexes, the H2/6 and H3/5 signals (in $CDCl_3$) appeared farther upfield with increasing basicity of the 4-Xpy ligand (Table 1). This trend can be attributed to the greater electron richness of the more basic 4-Xpy ligands. Plots of the chemical shift of the H2/6 signals of 4-Xpy and of *trans*-$[Pt^{II}(4\text{-Xpy})_2Cl_2]$ complexes versus the pK_a of 4-Xpy are linear and have a negative slope (Figure 6). For plots of both series of complexes in Figure 6, the order is as follows: 4-CNpy (**1**) > 4-CF_3py (**2**) > 4-MeCOpy (**6**) > 4-Mepy (**7**) > 4-MeOpy (**3**) > 4-Me_2Npy) (**4**) ≈ 4-$(CH_2)_5$Npy (**5**). The slightly steeper negative slope for the complexes than for the free ligand (Figure 6) can be attributed to the size of the synergistic decrease of the inductive effect of the Pt(II) metal center caused by the two mutually trans pyridyl rings. This decrease of the Pt(II) inductive effect is much smaller when the 4-Xpy ligand is a poor donor. Thus, H2/6 $\Delta\delta$ is larger. The H2/6 $\Delta\delta$ values decrease linearly with increasing pK_a of 4-Xpy from 0.35 to 0.11 ppm (Table 1 and Figure 7) in the same order as the plots in Figure 6.

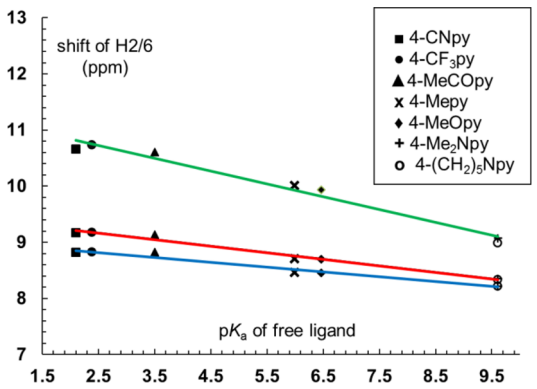

Figure 6. Shifts (ppm) of the H2/6 NMR signals (in $CDCl_3$, 25 °C) of 4-Xpy both free (5 mM, blue line; slope = −0.0856, R^2 = 0.972) and coordinated in *trans*-$[Pt(4\text{-Xpy})_2Cl_2]$ (5 mM, red line; slope = −0.1165, R^2 = 0.9862) and $[Pt(4\text{-Xpy})_4]Cl_2$ (5 mM, green line; slope = −0.2291, R^2 = 0.9789) plotted vs the pK_a of the free 4-Xpy. Data for "$[Pt(4\text{-Xpy})_4]Cl_2$" for X = CN, CF_3, and MeCO were obtained from the nitrate salt as explained in the text.

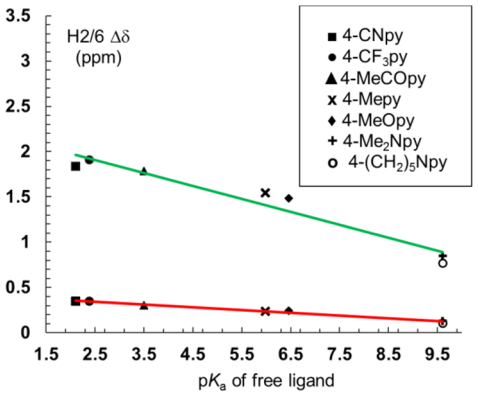

Figure 7. Change in shift ($\Delta\delta$, ppm) of the H2/6 ^{1}H NMR signal in $CDCl_3$ upon coordination of 4-Xpy to form *trans*-$[Pt(4\text{-Xpy})_2Cl_2]$ (red line; slope = −0.0305, R^2 = 0.9858) and $[Pt(4\text{-Xpy})_4]Cl_2$ (green line; slope = −0.1435, R^2 = 0.9449) plotted vs the pK_a of free 4-Xpy. Data for "$[Pt(4\text{-Xpy})_4]Cl_2$" for X = CN, CF_3, and MeCO were obtained from the nitrate salt as explained in the text.

Dependence of NMR Spectra (in $CDCl_3$) of $[Pt^{II}(4\text{-Xpy})_4]Cl_2$ Complexes on the Nature of X. As mentioned, side products having very downfield H2/6 signals found in early phases of this study were later identified as the $[Pt^{II}(4\text{-Xpy})_4]Cl_2$ salts. To obtain related products ($[Pt^{II}(4\text{-Xpy})_4]Y_2$) with poor donor 4-Xpy ligands, we used other poorly coordinating or non-coordinating counterions. Within any series of $[Pt^{II}(4\text{-Xpy})_4]Y_2$ complexes regardless of the identity of the Y counterion, the H2/6 and H3/5 signals appeared farther upfield with increasing basicity of the 4-Xpy ligands, as we found for the *trans*-$[Pt^{II}(4\text{-Xpy})_2Cl_2]$ complexes.

We begin the discussion with the $[Pt^{II}(4\text{-Xpy})_4]Cl_2$ complexes in $CDCl_3$ (Table 2), because we have the most extensive solution and structural data for the Y = Cl^- complexes and because $\Delta\delta$ is greater by ∼1 ppm when Y = Cl^- than when Y = other counterions; we conclude with a discussion of other solvents and $[Pt^{II}(4\text{-Xpy})_4]Y_2$ complexes with other Y counterions. In plots of the H2/6 shifts of $[Pt^{II}(4\text{-Xpy})_4]Cl_2$ and *trans*-$[Pt^{II}(4\text{-Xpy})_2Cl_2]$ in $CDCl_3$ versus the pK_a of 4-Xpy (Figure 6), the negative slope for the $[Pt^{II}(4\text{-Xpy})_4]Cl_2$ series is much steeper than for the *trans*-$[Pt^{II}(4\text{-Xpy})_2Cl_2]$ series. This observation can be interpreted as discussed above by noting that now there are four 4-Xpy ligands synergistically influencing the inductive effect of the Pt^{II} metal center and that the H2/6 shift is sensitive to this inductive effect. As a further illustration of the synergism, the $\Delta\delta$ values in $CDCl_3$ for $[Pt^{II}(4\text{-Xpy})_4]Cl_2$ (1.91−0.77 ppm, Table 2) decrease linearly with increasing pK_a of 4-Xpy (Figure 7) to a much greater extent than the *trans*-$[Pt^{II}(4\text{-Xpy})_2Cl_2]$ series.

DOI: 10.1021/acs.inorgchem.7b01294
Inorg. Chem. XXXX, XXX, XXX−XXX

The ^{1}H NMR shift data, especially for H2/6 at 8.84 ppm, reported by Pazderski et al.[23] $[Pt^{II}(py)_4]Cl_2$ in $CDCl_3$ do not agree at all with the H2/6 shifts (~10 ppm) observed here for the $[Pt^{II}(4\text{-Xpy})_4]Cl_2$ complexes with moderate donor 4-Xpy ligands (Table 2 and Supporting Information, Table S5). To independently verify the reported preparation[23] and characterization[44] of $[Pt^{II}(py)_4]Cl_2$ (**8a**), we prepared $[Pt^{II}(py)_4]Cl_2$ by our method and obtained colorless crystals with unit-cell parameters identical to those reported for $[Pt(py)_4]Cl_2$.[44] The H2/6 shift (10.36 ppm) in $CDCl_3$ at 25 °C for our $[Pt(py)_4]Cl_2$ crystals (see Supporting Information, Table S5) is entirely consistent with the shift value expected from our data. Concluding that some error was made in the previous work,[23] we turned our attention to elucidating the factors contributing to the very downfield position of these H2/6 signals.

Cause of the Unusually Large Downfield H2/6 Signals of $[Pt^{II}(4\text{-Xpy})_4]Cl_2$ Complexes. Understanding the specific factors causing the larger $\Delta\delta$ H2/6 values for $[Pt^{II}(4\text{-Xpy})_4]Cl_2$ salts than for salts with other counterions (Table 2) is an important goal of our study. Another interesting feature observed for the $[Pt^{II}(4\text{-Xpy})_4]Cl_2$ salts is their high solubility in $CDCl_3$, a solvent of low polarity. We believe that the $[Pt^{II}(4\text{-Xpy})_4]Cl_2$ solubility in $CDCl_3$ provides clear evidence that electrostatic attraction leads to the existence of $\{[Pt^{II}(4\text{-Xpy})_4]^{2+},2Cl^-\}$ ion pairs having overall low charge and containing multiple stabilizing (py)CH···Cl hydrogen bonds similar to those found in the solid state (Figure 5 and Supporting Information, Table S3).

We believe that there can be no doubt that ion pairs between the $[Pt^{II}(4\text{-Xpy})_4]^{2+}$ dication and the various Y anions do exist in the low-dielectric solvent $CDCl_3$. We hypothesize that in $CDCl_3$ solutions of $[Pt^{II}(4\text{-Xpy})_4]Cl_2$ complexes the close proximity of the Cl^- counterion to the H2/6 protons of the coordinated 4-Xpy pyridyl ring within such ion pairs results in the formation of multiple CH···Cl contacts between H2/6 and Cl^- and in dynamic ion pairs similar to the elongated pseudo-octahedrons found in the solid (Figure 5). The formation of hydrogen bonds is known to lead to downfield shift changes in the ^{1}H NMR signals.[50,51] Thus, the very downfield H2/6 signals for $[Pt^{II}(4\text{-Xpy})_4]Cl_2$ complexes in $CDCl_3$ are consistent with the presence of CH···Cl hydrogen bonds, proving beyond any doubt that specific cation−anion contacts exist within such dynamic ion pairs in solution is probably not possible, but we believe that the results of several solution studies to be described next lead to a very compelling case for the existence of *fully* formed $\{[Pt^{II}(4\text{-Xpy})_4]^{2+},2Cl^-\}$ ion pairs containing multiple CH···Cl interactions in $CDCl_3$.

To assess our hypothesis, we first examined the effect of $[Et_4N]Cl$ addition on the H2/6 signals of $[Pt^{II}(4\text{-Xpy})_4]Cl_2$ in $CDCl_3$ for X = MeO (**3a**), Me_2N (**4a**), $(CH_2)_5N$ (**5a**), and Me (**7a**). If the $\{[Pt^{II}(4\text{-Xpy})_4]^{2+},2Cl^-\}$ ion pairs were not fully formed, the H2/6 signal would shift downfield because the added chloride would drive the equilibrium toward the formation of more $\{[Pt^{II}(4\text{-Xpy})_4]^{2+},2Cl^-\}$ ion pairs. Downfield shifts are also expected if the ion pairs have only one chloride ion, $\{[Pt^{II}(4\text{-Xpy})_4]^{2+},Cl^-\}^+$. As the Cl^- concentration was increased, the H2/6 signals shifted slightly *upfield* by ~0.02 ppm for **3a** and **7a**, by 0.17 ppm for **4a**, and by 0.18 ppm for **5a** as up to 25 mM $[Et_4N]Cl$ was added (see Supporting Information, Figure S5). The absence of downfield shifts supports the proposal that $\{[Pt^{II}(4\text{-Xpy})_4]^{2+},2Cl^-\}$ ion pairs are already fully formed in the absence of added chloride salt. The minor upfield shifting is most consistent with salt effects.

A similar $[Et_4N]Cl$ salt effect study could not be conducted for $[Pt^{II}(4\text{-Xpy})_4]Cl_2$ complexes with the very weak donor 4-Xpy ligands (X = CN, CF_3, and MeCO) because the chloride salts could not be isolated. However, solutions containing $\{[Pt^{II}(4\text{-Xpy})_4]^{2+},2Cl^-\}$ ion pairs in $CDCl_3$ at 25 °C could be generated easily by adding $[Et_4N]Cl$ to suspensions of $[Pt^{II}(4\text{-Xpy})_4](NO_3)_2$ [X = CN (**1e**), CF_3 (**2e**), and MeCO (**6e**)] salts, which are insoluble or poorly soluble in $CDCl_3$; shift data from NMR spectra recorded within ~5 to 30 min after addition of $[Et_4N]Cl$ can be found in Table 2 and Figures 6 and 7. The $\Delta\delta$ values found for $\{[Pt^{II}(4\text{-Xpy})_4]^{2+},2Cl^-\}$ ion pairs (Table 2) are ~1.8 to 1.9 ppm when 4-Xpy is one of these poor ligands, as compared to $\Delta\delta \approx 1.5$ ppm for a medium donor ligand (e.g., X = Me) and $\Delta\delta < 0.9$ ppm for the stronger donor ligand (X = 4-Me_2N). These $\Delta\delta$ values are fully consistent with a decrease in the partial positive charge δ^+ of the H2/6 protons with increasing 4-Xpy pyridyl ring electron richness. A decrease in δ^+ of the H2/6 protons in turn diminishes the strength of the specific H2/6 H-bonding interactions with the chloride ion within the ion pair.

As an aside, as expected, NMR scans of these suspensions gave no or very weak signals (cf. Figure 8 for X = CN (**1e**)).

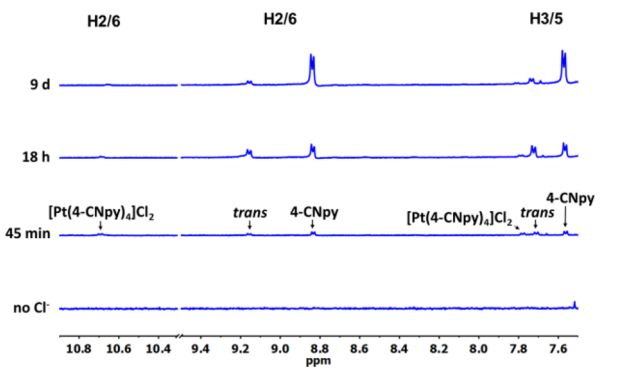

Figure 8. Stacked plot of the aromatic region of ^{1}H NMR spectra (in $CDCl_3$, 25 °C) for the treatment of $[Pt(4\text{-CNpy})_4](NO_3)_2$ (**1e**, 5 mM) with $[Et_4N]Cl$ (125 mM). Signals for the *trans*-$[Pt(4\text{-CNpy})_2Cl_2]$ complex are labeled *trans*. Procedures for obtaining spectra starting from such nitrate salts are explained in the text.

However, relatively soon after addition of $[Et_4N]Cl$ to $[Pt^{II}(4\text{-Xpy})_4](NO_3)_2$ (X = CN (**1e**), CF_3 (**2e**), and MeCO (**6e**)) suspensions in the studies just mentioned above, new signals corresponding to the free 4-Xpy ligand and to the *trans*-$[Pt^{II}(4\text{-Xpy})_2Cl_2]$ complex were detectable (see Figure 8 for X = CN (**1e**); also see Supporting Information, Figure S6). Scheme 2 describes the most likely course of the reactions.

Effect of $[Et_4N]Cl$ on the H2/6 Signals of $[Pt^{II}(4\text{-Xpy})_4](PF_6)_2$ and of $[Pt^{II}(4\text{-Mepy})_4]Y_2$ Complexes in $CDCl_3$ (X = MeO and $(CH_2)_5N$, and Y = PF_6^-, BF_4^-, and NO_3^-). In our studies of 5 mM solutions of $[Pt^{II}(4\text{-Xpy})_4]Y_2$ complexes in various solvents, we ranked the ability of the Y anions both to form ion pairs and to form hydrogen bonds as follows: $Cl^- > NO_3^- > BF_4^- \approx PF_6^-$. We begin by describing results leading to this order with our assessment of the effects of addition of $[Et_4N]Cl$ to $CDCl_3$ solutions of $[Pt^{II}(4\text{-Xpy})_4](PF_6)_2$ [X = MeO (**3b**), $(CH_2)_5N$ (**5b**), and Me (**7b**)] complexes. Such an addition was expected to convert a $\{[Pt^{II}(4\text{-Xpy})_4]^{2+},2PF_6^-\}$ ion pair to a $\{[Pt^{II}(4\text{-Xpy})_4]^{2+},2Cl^-\}$ ion pair. The change of

DOI: 10.1021/acs.inorgchem.7b01294
Inorg. Chem. XXXX, XXX, XXX−XXX

Scheme 2. Species Probably Formed (in CD_3CN and $CDCl_3$, 25 °C) after Addition of $[Et_4N]Cl$ to $[Pt(4\text{-}Xpy)_4](NO_3)_2$ Complexes in Which 4-Xpy is a Weak Donor Ligand

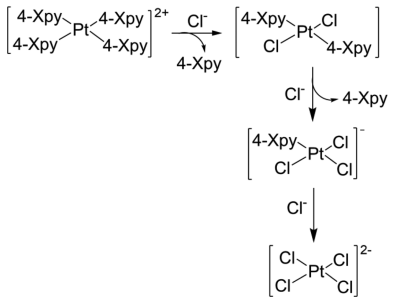

the counterion in the ion pair caused downfield shift changes of the H2/6 signals in $CDCl_3$ (Figure 9 and Supporting Information, Figure S7).

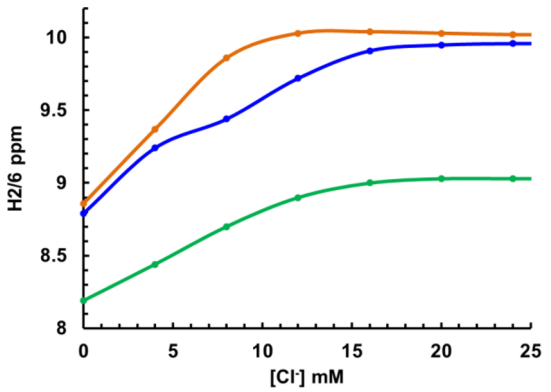

Figure 9. Shift of the H2/6 signal of $[Pt(4\text{-}Mepy)_4](PF_6)_2$ (**7b**, 5 mM, orange), $[Pt(4\text{-}MeOpy)_4](PF_6)_2$ (**3b**, 5 mM, blue), and $[Pt(4\text{-}(CH_2)_5Npy)_4](PF_6)_2$ (**5b**, 5 mM, green) upon addition of $[Et_4N]Cl$ (0–25 mM) in $CDCl_3$ at 25 °C.

The curves showing the dependence of the downfield shift changes of H2/6 signals for **7b** and **5b** on adding $[Et_4N]Cl$ have the smooth shape most often found in our studies (Figure 9 and Supporting Information, Figure S7). For **5b** (bearing the highly basic 4-$(CH_2)_5$Npy ligand), the $[Et_4N]Cl$ concentration (Figure 9 and Supporting Information, Figure S7) required to reach a plateau (~20 mM) was higher than that for **7b** (~12 mM), as expected, because 4-$(CH_2)_5$Npy in **5b** is much more electron-rich than is 4-Mepy in **7b**. Thus, the $\delta+$ charge on the H2/6 protons is relatively smaller, and the CH···Cl interactions within the ion pair are weaker for 4-$(CH_2)_5$Npy in **5b** than those for 4-Mepy in **7b**; a higher $[Cl^-]$ is therefore required by **5b** than by **7b** to fully form $\{[Pt^{II}(4\text{-}Xpy)_4]^{2+},2Cl^-\}$ ion pairs. The H2/6 signals for **7b** and **5b** initially at 8.86 and 8.22 ppm shifted downfield to 10.04 ppm at ~12 mM $[Cl^-]$ and 9.02 ppm at ~20 mM $[Cl^-]$, respectively (Figure 9 and Supporting Information, Figure S7). The shift change observed for **7b** (~1.2 ppm) was much larger than for $[Pt^{II}(4\text{-}(CH_2)_5Npy)_4](PF_6)_2$ (**5b**) (~0.8 ppm). The smaller H2/6 shift change observed for **5b**, bearing the highly basic 4-$(CH_2)_5$Npy ligand, can be attributed to the electron richness of the pyridyl ring, which in turn lowers the partial positive charge of the H2/6 protons and diminishes the hydrogen-bonding ability of these hydrogens. The results for solutions are consistent with the solid-state data; the average nonbonding (py)C–H···Cl distances observed for $[Pt^{II}(4\text{-}(CH_2)_5Npy)_4]Cl_2$ (**5a**) are slightly longer than those observed for $[Pt^{II}(4\text{-}Mepy)_4]Cl_2$ (**7a**) (Supporting Information). These comparative results for **7b** and **5b** are readily rationalized only if specific contacts occur between the Cl^- anion and the H2/6 protons in the ion pairs.

The curve of the shift changes observed for the H2/6 signal of $[Pt^{II}(4\text{-}MeOpy)_4]PF_6$ (**3b**) has a different shape than those found for **5b** and **7b**. This different shape was found in a few cases (Figure 9 and Supporting Information). Both **3b** and **7b** have moderately basic 4-Xpy ligands, and the starting and ending H2/6 shifts are very similar. Likewise, the H2/6 shift change upon addition of the first aliquot of ~5 mM Cl^- (~1 equiv of Cl^-) is similar for **3b** and **7b**. However, as more Cl^- was added, the chemical shift of the H2/6 signal of **3b** plateaued and then increased again, and finally plateaued at a shift similar to that of **7b**. Such a finding cannot be easily explained if there are no specific contacts in the ion pair. However, if the first equivalent of added Cl^- altered the canting angles within the $\{[Pt^{II}(4\text{-}MeOpy)_4]^{2+},Cl^-,PF_6^-\}$ ion pair, a higher amount of Cl^- would then be needed for a second Cl^- to fully displace the remaining PF_6^- from this ion pair to form the $\{[Pt^{II}(4\text{-}MeOpy)_4]^{2+},2Cl^-\}$ ion pair.

To assess the effect of counterions other than PF_6^- on Cl^- ion-pairing interactions with $[Pt^{II}(4\text{-}Xpy)_4]^{2+}$, $[Et_4N]Cl$ addition experiments using $[Pt^{II}(4\text{-}Mepy)_4](BF_4)_2$ (**7c**) and $[Pt^{II}(4\text{-}Mepy)_4](NO_3)_2$ (**7e**) were conducted (Figure 10 and

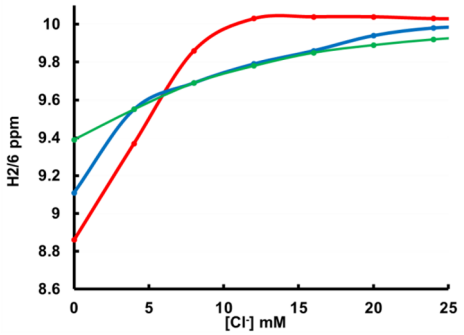

Figure 10. Shift of the H2/6 signal of $[Pt(4\text{-}Mepy)_4](PF_6)_2$ (**7b**, 5 mM, red), $[Pt(4\text{-}Mepy)_4](BF_4)_2$ (**7c**, 5 mM, blue), and $[Pt(4\text{-}Mepy)_4](NO_3)_2$ (**7e**, 5 mM, green) upon addition of $[Et_4N]Cl$ up to 25 mM in $CDCl_3$ at 25 °C.

Supporting Information, Figure S9). As the $[Et_4N]Cl$ concentration was increased from 0–125 mM, the H2/6 signals for **7c** and **7e** shifted downfield from 9.11 and 9.39 ppm to 10.02 and 10.00 ppm, respectively. The shift change of the H2/6 signal (~1.2 ppm) observed for $[Pt^{II}(4\text{-}Mepy)_4](PF_6)_2$ (**7b**) was more than that observed for **7c** (~0.9 ppm) and **7e** (~0.6 ppm, in $CDCl_3$ at 25 °C). The concentration of $[Et_4N]Cl$ required to reach a plateau was much lower (~13 mM) for **7b** (with the PF_6^- anion) than for **7c** (~25 mM) or **7e** (~50 mM) (with the BF_4^- or NO_3^- counterions, respectively). Of greater interest, the curve for **7c** rose sharply to an ~1:1 ratio of Cl^-, and then rose more gradually. This curve indicates that very likely a mixed $\{[Pt^{II}(4\text{-}Mepy)_4]^{2+},Cl^-,BF_4^-\}$ ion pair forms readily with one Cl^- and one BF_4^-, as proposed above for the $\{[Pt^{II}(4\text{-}MeOpy)_4]^{2+},Cl^-,PF_6^-\}$ ion pair. Perhaps the H-bonding interactions within the $\{[Pt^{II}(4\text{-}Xpy)_4]^{2+},Cl^-,BF_4^-\}$ ion pair causes changes in the canting of the bound 4-Mepy ligands. The solid-state structural data show that large changes in canting are feasible. Such a change in canting could favor H-

DOI: 10.1021/acs.inorgchem.7b01294
Inorg. Chem. XXXX, XXX, XXX–XXX

bonding by the tetrahedral BF_4^- remaining in the mixed ion pair. The BF_4^- could then be more difficult to substitute from the mixed ion pair than the octahedral PF_6^- in the $\{[Pt^{II}(4\text{-}Xpy)_4]^{2+},Cl^-,PF_6^-\}$ ion pair. In any case, the shape of the curve is further evidence that there are specific contacts within these ion pairs. The interaction of the Y anions with the H2/6 protons in $\{[Pt^{II}(4\text{-}Xpy)_4]^{2+},2Y^-\}$ ion pairs thus decreases in the order: $Cl^- > NO_3^- > BF_4^- \approx PF_6^-$.

Shift of the H2/6 Signals of $[Pt^{II}(4\text{-}Xpy)_4](NO_3)_2$ and Other $[Pt^{II}(4\text{-}Xpy)_4]Y_2$ Complexes in CD_3CN. When the counterion is not chloride, $[Pt^{II}(4\text{-}Xpy)_4]Y_2$ salts are often not soluble in $CDCl_3$ (cf. Table 2). We decided to conduct broader studies in the more polar solvents in the hope that we could obtain data relevant to ion pairing on more $[Pt^{II}(4\text{-}Xpy)_4]Y_2$ compounds in a given solvent. Because D_2O and DMSO-d_6 are too polar to allow extensive ion pairing (Supporting Information), we chose to explore CD_3CN. All $[Pt^{II}(4\text{-}Xpy)_4]Y_2$ complexes prepared in this study were soluble at 5 mM concentration in CD_3CN. This solvent was polar enough to allow NMR spectra to be recorded at 25 °C but was not so polar as to preclude formation of ion pairs (Tables 3 and S8). Furthermore, addition of $[Et_4N]Cl$ to the chloride salt, $[Pt^{II}(4\text{-}Me_2Npy)_4]Cl_2$ (**4a**), in CD_3CN caused a downfield shift of 0.33 ppm of the H2/6 signal (Table 3). This finding indicates that the ion pair is not fully formed in CD_3CN. In contrast, $[Et_4N]Cl$ addition to **4a** and other chloride salts in $CDCl_3$ led to upfield H2/6 shifts (Figure S5), indicating that the ion pair was fully formed in the less polar $CDCl_3$ solvent.

^1H NMR spectra of $[Pt^{II}(4\text{-}Xpy)_4](NO_3)_2$ CD_3CN solutions were recorded ~5 min after addition of sufficient $[Et_4N]Cl$ to make the solutions 50.0 mM in $[Et_4N]Cl$. For all five complexes studied, downfield H2/6 shift changes were observed as expected (Table 3, Figure 11, and Supporting Information, Figures S10–S12). The H2/6 shift changes observed for $[Pt^{II}(4\text{-}CNpy)_4](NO_3)_2$ (~1.2 ppm), $[Pt^{II}(4\text{-}CF_3py)_4](NO_3)_2$ (~1.1 ppm), $[Pt^{II}(4\text{-}MeCOpy)_4](NO_3)_2$ (~1.2 ppm), and $[Pt^{II}(4\text{-}MeOpy)_4](NO_3)_2$ (~1.2 ppm) were greater than the 0.75 ppm observed for $[Pt^{II}(4\text{-}Me_2Npy)_4](NO_3)_2$ (Table 3). Such larger H2/6 shift changes indicate that H bonding to Cl is better when 4-Xpy is a poor or moderate donor with low pyridyl-ring electron richness and hence greater partial positive charge, δ^+, on the H2/6 protons. Thus, ion pairs with specific interactions in CD_3CN are similar in nature to those in $CDCl_3$, although CD_3CN is more polar.

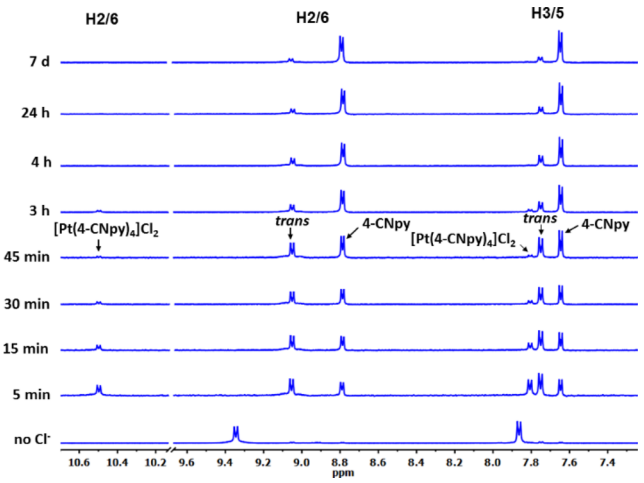

Figure 11. Stacked plot of the aromatic region of ^1H NMR spectra (in CD_3CN, 25 °C) for the treatment of $[Pt(4\text{-}CNpy)_4](NO_3)_2$ (**1e**, 5 mM) with $[Et_4N]Cl$ (50 mM). Signals for *trans*-$[Pt(4\text{-}CNpy)_2Cl_2]$ are labeled *trans*.

^1H NMR signals of "free" 4-Xpy and *trans*-$[Pt^{II}(4\text{-}Xpy)_2Cl_2]$ in the first spectrum recorded (~5 min) after $[Et_4N]Cl$ addition to $[Pt^{II}(4\text{-}CNpy)_4](NO_3)_2$ (**1e**), $[Pt^{II}(4\text{-}CF_3py)_4](NO_3)_2$ (**2e**), and $[Pt^{II}(4\text{-}MeCOpy)_4](NO_3)_2$ (**6e**) in CD_3CN at 25 °C (Figure 11 and Supporting Information, Figures S10–S12). Less time was required for the intensity of the aromatic signals of $[Pt^{II}(4\text{-}CNpy)_4]Cl_2$ (~4 h) and $[Pt^{II}(4\text{-}MeCOpy)_4]Cl_2$ (~6 h) to reach the baseline than in the case of $[Pt^{II}(4\text{-}CF_3py)_4]Cl_2$ (~24 h). Therefore, the donor ability of 4-Xpy decreases in the order X = CF_3 > CN ≈ MeCO. For a detailed discussion of the spectral changes over time, see Supporting Information.

CONCLUSIONS

The dependence of the chemical shifts of 4-Xpy H2/6 ^1H NMR signals of many new complexes in two series, namely, *trans*-$[Pt^{II}(4\text{-}Xpy)_2Cl_2]$ and $[Pt^{II}(4\text{-}Xpy)_4]Y_2$, were investigated by employing 4-Xpy with very diverse donor abilities. For both series in $CDCl_3$, downfield shift changes ($\Delta\delta$) were observed for the H2/6 signals upon coordination of 4-Xpy to form the respective *trans*-$[Pt^{II}(4\text{-}Xpy)_2Cl_2]$ or $[Pt(4\text{-}Xpy)_4]Cl_2$ complexes. The size of H2/6 $\Delta\delta$ decreased linearly with increasing 4-Xpy donor ability. The decrease in $\Delta\delta$ was greater for the $[Pt(4\text{-}Xpy)_4]Cl_2$ series than for the *trans*-$[Pt^{II}(4\text{-}Xpy)_2Cl_2]$ series. We conclude that this finding can be attributed to the synergistic reduction in the inductive effect of the Pt(II) center by the other three 4-Xpy donor ligands in the $[Pt(4\text{-}Xpy)_4]Cl_2$ series as compared to only one other 4-Xpy donor ligand in the *trans*-$[Pt^{II}(4\text{-}Xpy)_2Cl_2]$ series.

Solutions of $[Pt(4\text{-}Xpy)_4]Cl_2$ salts in $CDCl_3$ have very downfield 4-Xpy H2/6 ^1H NMR signals and exhibit much larger H2/6 $\Delta\delta$ values than those of the corresponding $[Pt^{II}(4\text{-}Xpy)_4]Y_2$ (Y = PF_6, BF_4, and NO_3) salts. We conclude that strong ion pairing between Cl^- and $[Pt^{II}(4\text{-}Xpy)_4]^{2+}$ is facilitated by multiple H2/6···Cl^- H-bonding contacts, explaining the large downfield shifts. Also, strong ion pairing explains the high solubility of the $[Pt^{II}(4\text{-}Xpy)_4]Cl_2$ salts that contain a $[Pt^{II}(4\text{-}Xpy)_4]^{2+}$ dication. Other $[Pt^{II}(4\text{-}Xpy)_4]Y_2$ salts were often much less soluble or even insoluble. Crystal structures revealed that the chloride counterions occupy axial positions with nonbonding (py)C–H···Cl distances well within the range of a typical CH···Cl H-bonding contact (2.4–3.0 Å). Thus, the crystallographic data confirm our conclusion that the relatively larger H2/6 $\Delta\delta$ values (in $CDCl_3$ at 25 °C) observed for $[Pt^{II}(4\text{-}Xpy)_4]Cl_2$ arise from ion pairing, which in turn is stabilized by multiple (py)C–H···Cl contacts.

Several ^1H NMR studies in various solvents allowed us to correlate the dependence of the relative stability of the ion pairs of $[Pt^{II}(4\text{-}Xpy)_4]Y_2$ based on their H-bonding ability as follows: $Cl^- > NO_3^- > BF_4^- > PF_6^-$. The poor solubility of some $[Pt^{II}(4\text{-}Xpy)_4]Y_2$ (Y = PF_6, BF_4, and NO_3) complexes as compared to the $[Pt^{II}(4\text{-}Xpy)_4]Cl_2$ analogues is probably a result of the weaker ion pairing.

Because our procedures for synthesizing model *trans*-$[Pt^{II}(4\text{-}Xpy)_2Cl_2]$ and $[Pt^{II}(4\text{-}Xpy)_4]Y_2$ complexes do not rely on high temperatures, water solubility, or Xpy volatility, the methods are clearly applicable to other nonvolatile monodentate ligands, such as those bearing biological targeting groups. The NMR spectroscopic trends we have elucidated can serve as a guide

DOI: 10.1021/acs.inorgchem.7b01294
Inorg. Chem. XXXX, XXX, XXX–XXX

during the synthesis and characterization of such Pt(II) complexes.

■ ASSOCIATED CONTENT

Supporting Information

The Supporting Information is available free of charge on the ACS Publications website at DOI: 10.1021/acs.inorgchem.7b01294.

Details of the syntheses and characterization of all complexes prepared in this study; descriptions and figures of the effect of $[Et_4N]Cl$ addition on ^1H NMR signals of $[Pt^{II}(4\text{-Xpy})_4]Y_2$ in various solvents; descriptions and figures of replacement of weak 4-Xpy ligands by chloride upon $[Et_4N]Cl$ addition to $[Pt^{II}(4\text{-Xpy})_4](NO_3)_2$ suspensions or solutions; tables of crystallographic data for complexes **2**, **3**, **4′**, **5**, **3a**, **4a**, **5a**, and **7a** in CIF format; tables of selected nonbonding Pt···Cl and (py)C−H···Cl distances and dihedral angles; tables of ^1H NMR data in $CDCl_3$ for py and various Pt(II) py complexes and for *trans*-$[Pt(4\text{-Xpy})_2Cl_2]$ complexes; tables of ^1H NMR shift data in $CDCl_3$, CD_3CN, DMSO-d_6, and D_2O for free 4-Xpy and for $[Pt(4\text{-Xpy})_4]Y_2$ complexes both with and without added $[Et_4N]Cl$; figure showing the orientation of the pyridyl rings relative to the coordination plane in *cis*-$[Pt(4\text{-Me}_2\text{Npy})_2Cl_2]$; plots of ^1H NMR data versus pK_a for free ligand and for *trans*-$[Pt(4\text{-Xpy})_2Cl_2]$ (including X = H) in $CDCl_3$ (PDF)

Accession Codes

CCDC 1551057−1551064 contain the supplementary crystallographic data for this paper. These data can be obtained free of charge via www.ccdc.cam.ac.uk/data_request/cif, or by emailing data_request@ccdc.cam.ac.uk, or by contacting The Cambridge Crystallographic Data Centre, 12 Union Road, Cambridge CB2 1EZ, UK; fax: +44 1223 336033.

■ AUTHOR INFORMATION

Corresponding Author

*E-mail: lmarzil@lsu.edu.

ORCID

Patricia A. Marzilli: 0000-0002-8103-9606

Luigi G. Marzilli: 0000-0002-0406-0858

Notes

The authors declare no competing financial interest.

■ ACKNOWLEDGMENTS

Upgrade of the diffractometer was made possible through Grant No. LEQSF(2011-12)-ENH-TR-01, administered by the Louisiana Board of Regents.

■ REFERENCES

(1) Lewis, N. A.; Marzilli, P. A.; Fronczek, F. R.; Marzilli, L. G. Models for B_{12}-Conjugated Radiopharmaceuticals. Cobaloxime Binding to New fac-$[Re(CO)_3(Me_2Bipyridine)(Amidine)]BF_4$ Complexes Having an Exposed Pyridyl Nitrogen. *Inorg. Chem.* **2014**, *53* (20), 11096−11107.

(2) Kelland, L. The Resurgence of Platinum-Based Cancer Chemotherapy. *Nat. Rev. Cancer* **2007**, *7* (8), 573−584.

(3) Wilson, J. J.; Lippard, S. J. In Vitro Anticancer Activity of *cis*-Diammineplatinum(II) Complexes with *β*-Diketonate Leaving Group Ligands. *J. Med. Chem.* **2012**, *55* (11), 5326−5336.

(4) Jakupec, M. A.; Galanski, M.; Arion, V. B.; Hartinger, C. G.; Keppler, B. K. Antitumor Metal Compounds: More Than Theme and Variations. *Dalton Trans.* **2008**, *2*, 183−194.

(5) Wheate, N. J.; Walker, S.; Craig, G. E.; Oun, R. The Status of Platinum Anticancer Drugs in the Clinic and in Clinical Trials. *Dalton Trans.* **2010**, *39* (35), 8113−8127.

(6) Klein, A. V.; Hambley, T. W. Platinum Drug Distribution in Cancer Cells and Tumors. *Chem. Rev.* **2009**, *109* (10), 4911−4920.

(7) Warad, I.; Eftaiha, A. a. F.; Al-Nuri, M. A.; Husein, A. I.; Assal, M.; Abu-Obaid, A.; Al-Zaqri, N.; Ben Hadda, T.; Hammouti, B. Metal Ions as Antitumor Complexes - Review. *J. Mater. Environ. Sci.* **2013**, *4* (4), 542−557.

(8) Kalinowska-Lis, U.; Ochocki, J.; Matlawska-Wasowska, K. Trans Geometry in Platinum Antitumor Complexes. *Coord. Chem. Rev.* **2008**, *252* (12−14), 1328−1345.

(9) Li, C.; Huang, R.-R.; Ding, Y.; Sletten, E.; Arnesano, F.; Losacco, M.; Natile, G.; Liu, Y.-Z. Effect of Thioethers on DNA Platination by *Trans*-Platinum Complexes. *Inorg. Chem.* **2011**, *50* (17), 8168−8176.

(10) Aleman, J.; del Solar, V.; Cubo, L.; Quiroga, A. G.; Navarro Ranninger, C. New Reactions of Anticancer-Platinum Complexes and their Intriguing Behaviour Under Various Experimental Conditions. *Dalton Trans.* **2010**, *39* (44), 10601−10607.

(11) Coluccia, M.; Natile, G. *Trans*-Platinum Complexes in Cancer Therapy. *Anti-Cancer Agents Med. Chem.* **2007**, *7* (1), 111−123.

(12) Li, C.; Ding, Y.; Cheng, L.; Zheng, Y.; Sletten, E.; Liu, Y. Effects of Buffers and pH on the Reaction of a *Trans*-Platinum Complex with 5′-Guanosine Monophosphate. *Eur. J. Inorg. Chem.* **2015**, *2015*, 4914−4920.

(13) Coluccia, M.; Nassi, A.; Loseto, F.; Boccarelli, A.; Mariggio, M. A.; Giordano, D.; Intini, F. P.; Caputo, P.; Natile, G. A *Trans*-Platinum Complex Showing Higher Antitumor Activity than the *Cis* Congeners. *J. Med. Chem.* **1993**, *36*, 510−512.

(14) Montero, E. I.; Diaz, S.; Gonzalez-Vadillo, A. M.; Perez, J. M.; Alonso, C.; Navarro-Ranninger, C. Preparation and Characterization of Novel *trans*-$[PtCl_2(Amine)(Isopropylamine)]$ Compounds: Cytotoxic Activity and Apoptosis Induction in Ras-Transformed Cells. *J. Med. Chem.* **1999**, *42* (20), 4264−4268.

(15) Aris, S. M.; Farrell, N. P. Towards Antitumor Active *Trans*-Platinum Compounds. *Eur. J. Inorg. Chem.* **2009**, *2009*, 1293−1302.

(16) Filipovic, L.; Arandelovic, S.; Gligorijevic, N.; Krivokuca, A.; Jankovic, R.; Srdic-Rajic, T.; Rakic, G.; Tesic, Z.; Radulovic, S. Biological Evaluation of *Trans*-Dichloridoplatinum(II) Complexes with 3- and 4-Acetylpyridine in Comparison to Cisplatin. *Radiol. Oncol.* **2013**, *47* (4), 346−357.

(17) Rakic, G. M.; Grguric-Sipka, S.; Kaluderovic, G. N.; Gomez-Ruiz, S.; Bjelogrlic, S. K.; Radulovic, S. S.; Tesic, Z. L. Novel *Trans*-Dichloroplatinum(II) Complexes with 3- and 4-Acetylpyridine: Synthesis, Characterization, DFT Calculations and Cytotoxicity. *Eur. J. Med. Chem.* **2009**, *44* (5), 1921−1925.

(18) Leng, M.; Locker, D.; Giraud-Panis, M.-J.; Schwartz, A.; Intini, F. P.; Natile, G.; Pisano, C.; Boccarelli, A.; Giordano, D.; Coluccia, M. Replacement of an NH_3 by an Iminoether in Transplatin makes an Antitumor Drug from an Inactive Compound. *Mol. Pharmacol.* **2000**, *58* (6), 1525−1535.

(19) Saad, J. S.; Benedetti, M.; Natile, G.; Marzilli, L. G. Basic Coordination Chemistry Relevant to DNA Adducts Formed by the Cisplatin Anticancer Drug. NMR Studies on Compounds with Sterically Crowded Chiral Ligands. *Inorg. Chem.* **2010**, *49* (12), 5573−5583.

(20) Saad, J. S.; Benedetti, M.; Natile, G.; Marzilli, L. G. NMR Studies of Models Having the Pt(d(GpG)) 17-Membered Macrocyclic Ring Formed in DNA by Platinum Anticancer Drugs: Pt Complexes with Bulky Chiral Diamine Ligands. *Inorg. Chem.* **2011**, *50* (10), 4559−4571.

(21) Andrepont, C.; Marzilli, P. A.; Marzilli, L. G. Guanine Nucleobase Adducts Formed by [Pt(di-(2-picolyl)amine)Cl]Cl: Evidence That a Tridentate Ligand with Only in-Plane Bulk Can Slow Guanine Base Rotation. *Inorg. Chem.* **2012**, *51* (21), 11961−11970.

DOI: 10.1021/acs.inorgchem.7b01294
Inorg. Chem. XXXX, XXX, XXX−XXX

(22) Andrepont, C.; Marzilli, P. A.; Pakhomova, S.; Marzilli, L. G. Guanine Nucleobase Adducts Formed by a Monofunctional Complex: [Pt(N-(6-methyl-2-picolyl)-N-(2-picolyl)amine)Cl]Cl. *J. Inorg. Biochem.* **2015**, *153*, 219−230.
(23) Pazderski, L.; Szlyk, E.; Sitkowski, J.; Kamienski, B.; Kozerski, L.; Tousek, J.; Marek, R. Experimental and Quantum-Chemical Studies of ^{15}N NMR Coordination Shifts in Palladium and Platinum Chloride Complexes with Pyridine, 2,2′-Bipyridine and 1,10-Phenanthroline. *Magn. Reson. Chem.* **2006**, *44* (2), 163−170.
(24) Tessier, C.; Rochon, F. D. Multinuclear NMR Study and Crystal Structures of Complexes of the Types Cis- and Trans-Pt(Ypy)$_2$X$_2$, where Ypy = Pyridine Derivative and X = Cl and I. *Inorg. Chim. Acta* **1999**, *295* (1), 25−38.
(25) Thompson, L. K. Trans Platinum(II) Complexes with Pyridine and Substituted Pyridines. *Inorg. Chim. Acta* **1980**, *38*, 117−119.
(26) Kauffman, G. B.; Thompson, R. J.cis- and trans-Dichloro-(dipyridine)Platinum(II). In *Inorganic Syntheses;* John Wiley & Sons, Inc.: Hoboken, NJ, 1963; Vol. *7*, pp 249−253.
(27) Pazderski, L.; Tousek, J.; Sitkowski, J.; Malinakova, K.; Kozerski, L.; Szlyk, E. Experimental and Quantum-Chemical Studies of ^{1}H, ^{13}C and ^{15}N NMR Coordination Shifts in Au(III), Pd(II) and Pt(II) Chloride Complexes with Picolines. *Magn. Reson. Chem.* **2009**, *47* (3), 228−238.
(28) Perera, T.; Abhayawardhana, P.; Marzilli, P. A.; Fronczek, F. R.; Marzilli, L. G. Formation of a Metal-to-Nitrogen Bond of Normal Length by a Neutral Sufonamide Group within a Tridentate Ligand. A New Approach to Radiopharmaceutical Bioconjugation. *Inorg. Chem.* **2013**, *52* (5), 2412−2421.
(29) Saad, J. S.; Marzilli, P. A.; Intini, F. P.; Natile, G.; Marzilli, L. G. Single-Stranded Oligonucleotide Adducts Formed by Pt Complexes Favoring Left-Handed Base Canting: Steric Effect of Flanking Residues and Relevance to DNA Adducts Formed by Pt Anticancer Drugs. *Inorg. Chem.* **2011**, *50* (17), 8608−8620.
(30) Andrepont, C.; Pakhomova, S.; Marzilli, P. A.; Marzilli, L. G. Unusual Example of Chelate Ring Opening Upon Coordination of the 9-Ethylguanine Nucleobase to [Pt(di-(6-methyl-2-picolyl)amine)Cl]-Cl. *Inorg. Chem.* **2015**, *54* (10), 4895−4908.
(31) Thompson, L. K. Trans Platinum(II) Complexes with Pyridine and Substituted Pyridines. *Inorg. Chim. Acta* **1980**, *38* (1), 117−119.
(32) Watt, G. W.; Thompson, L. K.; Pappas, A. J. Tetrakis and Bis Platinum(II) Iodide Complexes with Pyridine and Substituted-Pyridine Ligands. *Inorg. Chem.* **1972**, *11* (4), 747−749.
(33) Sokolenko, V. A.; Bondarenko, V. S.; Korniets, E. D.; Kovtonyuk, N. P.; Kovrova, N. B. Solid-Phase Condensation of Coordinated Pyridine and γ-Picoline in Patinum(II) Complexes. *Zh. Neorg. Khim.* **1989**, *34* (6), 1537−1540.
(34) Bondarenko, V. S.; Korniets, E. D.; Sokolenko, V. A.; Kovrova, N. B.; Kovtonyuk, N. P. Thermolysis of Platinum(IV) Complexes of Pyridine and γ-Picoline. *Zh. Neorg. Khim.* **1989**, *34* (6), 1541−1543.
(35) Pazderski, L.; Pawlak, T.; Sitkowski, J.; Kozerski, L.; Szlyk, E. Structural Correlations for ^{1}H, ^{13}C and ^{15}N NMR Coordination Shifts in Au(III), Pd(II) and Pt(II) Chloride Complexes with Lutidines and Collidine. *Magn. Reson. Chem.* **2010**, *48* (6), 417−426.
(36) Hambley, T. W. van der Waals Radii of Pt(II) and Pd(II) in Molecular Mechanics Models and an Analysis of Their Relevance to the Description of Axial M···H(-C), M···H(-N), M···S, and M···M (M = Pd(II) or Pt(II)) Interactions. *Inorg. Chem.* **1998**, *37* (15), 3767−3774.
(37) Bondi, A. Van der Waals Volumes and Radii. *J. Phys. Chem.* **1964**, *68* (3), 441−451.
(38) Price, J. H.; Williamson, A. N.; Schramm, R. F.; Wayland, B. B. Palladium(II) and Platinum(II) Alkyl Sulfoxide Complexes. Examples of Sulfur-Bonded, Mixed Sulfur- and Oxygen-Bonded, and Totally Oxygen-Bonded Complexes. *Inorg. Chem.* **1972**, *11* (6), 1280−1284.
(39) Sheldrick, G. M. *SADABS;* University of Göttingen: Germany, 1997.
(40) Sheldrick, G. M. A Short History of SHELX. *Acta Crystallogr., Sect. A: Found. Crystallogr.* **2008**, *A64*, 112−122.
(41) Colamarino, P.; Orioli, P. L. Crystal and Molecular Structures of *Cis*- and Trans-Dichlorobis(pyridine)Platinum(II). *J. Chem. Soc., Dalton Trans.* **1975**, *16−17*, 1656−1659.
(42) Maheshwari, V.; Bhattacharyya, D.; Fronczek, F. R.; Marzilli, P. A.; Marzilli, L. G. Chemistry of HIV-1 Virucidal Pt Complexes Having Neglected Bidentate sp2 N-Donor Carrier Ligands with Linked Triazine and Pyridine Rings. Synthesis, NMR Spectral Features, Structure, and Reaction with Guanosine. *Inorg. Chem.* **2006**, *45* (18), 7182−7190.
(43) Pitteri, B.; Marangoni, G.; Cattalini, L.; Visentin, F.; Bertolasi, V.; Gilli, P. The Role of the Non-Participating Groups in Substitution Reactions at Cationic Pt(II) Complexes Containing Tridentate Chelating Nitrogen Donors. Crystal Structure of {Pt[bis(2-pyridylmethyl)amine](py)}(CF$_3$SO$_3$)$_2$. *Polyhedron* **2001**, *20* (9−10), 869−880.
(44) Wei, C. H.; Hingerty, B. E.; Busing, W. R. Structure of Tetrakis(pyridine)Platinum(II) Chloride Trihydrate: Unconstrained Anisotropic Least-Squares Rrefinement of Hydrogen and Non Hydrogen Atoms from Combined X-Ray-Neutron Diffraction Data. *Acta Crystallogr., Sect. C: Cryst. Struct. Commun.* **1989**, *C45* (1), 26−30.
(45) de Medeiros, V. C.; de Andrade, R. B.; Leitao, E. F. V.; Ventura, E.; Bauerfeldt, G. F.; Barbatti, M.; do Monte, S. A. Photochemistry of CH_3Cl: Dissociation and CH···Cl Hydrogen Bond Formation. *J. Am. Chem. Soc.* **2016**, *138* (1), 272−280.
(46) Thallapally, P. K.; Nangia, A. A Cambridge Structural Database Analysis of the C-H···Cl Interaction: C-H···Cl- and C-H···Cl-M often Behave as Hydrogen Bonds but C-H···Cl-C is Generally a Van der Waals Interaction. *CrystEngComm* **2001**, *3*, 1−6.
(47) Thallapally, P. K.; Nangia, A. A Cambridge Structural Database Analysis of the C-H···Cl Interaction: C-H···Cl$^-$ and C-H···Cl-M Often Behave as Hydrogen Bonds but C-H···Cl-C is Generally a Van der Waals Interaction. *CrystEngComm* **2001**, *3* (27), 114−119.
(48) Aakeroy, C. B.; Evans, T. A.; Seddon, K. R.; Palinko, I. The C-H···Cl Hydrogen Bond: Does it Exist? *New J. Chem.* **1999**, *23* (2), 145−152.
(49) Bresciani-Pahor, N.; Forcolin, M.; Marzilli, L. G.; Randaccio, L.; Summers, M. F.; Toscano, P. J. Organocobalt B_{12} Models: Axial Ligand Effects on the Structural and Coordination Chemistry of Cobaloximes. *Coord. Chem. Rev.* **1985**, *63*, 1−125.
(50) Hibbert, F.; Emsley, J. Hydrogen Bonding and Chemical Reactivity. *Adv. Phys. Org. Chem.* **1990**, *26*, 255−279.
(51) Konrat, R.; Tollinger, M.; Kontaxis, G.; Krautler, B. NMR Techniques to Study Hydrogen Bonding in Aqueous Solution. *Monatsh. Chem.* **1999**, *130* (8), 961−982.
(52) Stilinovic, V.; Kaitner, B. Salts and Co-Crystals of Gentisic Acid with Pyridine Derivatives: The Effect of Proton Transfer on the Crystal Packing (and Vice Versa). *Cryst. Growth Des.* **2012**, *12* (11), 5763−5772.
(53) Bortoluzzi, M.; Annibale, G.; Marangoni, G.; Paolucci, G.; Pitteri, B. ^{31}P NMR and DFT Studies on Square-Planar Bis-(Diphenylphosphinoethyl)Phenylphosphine (Triphos) Complexes of Pt(II) with Pyridines and Anilines. *Polyhedron* **2006**, *25* (9), 1979−1984.
(54) Scriven, E. F. V.; Murugan, R. *Kirk-Othmer Encyclopedia of Chemical Technology;* John Wiley & Sons, Inc.: Hoboken, NJ, 2006; Vol. *21*, pp 91−133.
(55) Dawson, R. M. C. *Data for Biochemical Research,* 3rd ed.; Oxford Science Publications: Oxford, England, 1986; p 580.
(56) Honda, H. ^{1}H-MAS-NMR Chemical Shifts in Hydrogen-Bonded Complexes of Chlorophenols (Pentachlorophenol, 2,4,6-Trichlorophenol, 2,6-Dichlorophenol, 3,5-Dichlorophenol, and *p*-Chlorophenol) and Amine, and H/D Isotope Effects on ^{1}H-MAS-NMR Spectra. *Molecules* **2013**, *18*, 4786−4802.

DOI: 10.1021/acs.inorgchem.7b01294
Inorg. Chem. XXXX, XXX, XXX−XXX